# Modeling and Analysis of Inter-vehicle Communication: A Stochastic Geometry Approach

Thesis by

**Muhammad Junaid Farooq**

In Partial Fulfillment of the Requirements

For the Degree of

**Masters of Science**

*Electrical Engineering*

King Abdullah University of Science and Technology, Thuwal,

Kingdom of Saudi Arabia

April, 2015

The thesis of Muhammad Junaid Farooq is approved by the examination committee

Committee Chairperson: Dr. Mohamed-Slim Alouini

Committee Member: Dr. Tareq AlNaffouri

Committee Member: Dr. Marc G. Genton

# ABSTRACT


## Modeling and Analysis of Inter-vehicle Communication: A Stochastic Geometry Approach

Muhammad Junaid Farooq

Vehicular communication is the enabling technology for the development of the intelligent transportation systems (ITS), which aims to improve the efficiency and safety of transportation. It can be used for a variety of useful applications such as adaptive traffic control, coordinated braking, emergency messaging, peer-to-peer networking for infotainment services and automatic toll collection etc... Accurate yet simple models for vehicular networks are required in order to understand and optimize their operation. For reliable communication between vehicles, the spectrum access is coordinated via carrier sense multiple access (CSMA) protocol. Existing models either use a simplified network abstraction and access control scheme for analysis or depend on simulation studies. Therefore it is important to develop an analytical model for CSMA coordinated communication between vehicles.

In the first part of the thesis, stochastic geometry is exploited to develop a modeling framework for CSMA coordinated inter-vehicle communication (IVC) in a multi-lane highway scenario. The performance of IVC is studied in multi-lane highways taking into account the inter-lane separations and the number of traffic lanes and it is shown that for wide multi-lane highways, the line abstraction model that is widely used in literature loses accuracy and hence the analysis is not reliable. Since the pres-

ence of CSMA in the vehicular setting makes the analysis intractable, an aggressive interference approximation and a conservative interference approximation is proposed for the probability of transmission success. These approximations are tight in the low traffic and high traffic densities respectively.

In the subsequent part of the thesis, the developed model is extended to multi-hop IVC because several vehicular applications require going beyond the local communication and efficiently disseminate information across the roads via multi-hops. Two well-known greedy packet forwarding schemes are studied, that impose different tradeoffs between per-hop transmission success probability and forward packet progress, namely, the most forward with fixed radius (MFR) and the nearest with forward progress (NFP). In particular, a tractable and accurate modeling framework is developed to characterize the per-hop transmission success probability and the average forward progress for vehicular networks in a multi-lane highway setup. The developed model reveals the interplay between the spectrum sensing threshold of the CSMA protocol and the packet forwarding scheme. A new performance metric is defined, denoted as the aggregate packet progress (APP), which is a dimensionless quantity that captures the tradeoffs between the spatial frequency reuses efficiency, the per-hop transmission success probability, and the per-hop forward progress of the packets. To this end, in contrary to existing studies, the results show that with proper manipulation of CSMA threshold, the MFR achieves the highest APP.

# ACKNOWLEDGEMENTS

I would first like to thank Allah , Almighty who has helped me, guided me and gave me the strength to complete this work. Next, I would like to thank my thesis advisor, Prof. Mohamed-Slim Alouini for his tremendous support and advice throughout my Masters degree at KAUST, particularly under the most difficult times. I would also like to thank Dr. Hesham ElSawy, post doctoral fellow at KAUST, for his mentorship, assistance and sincere advice in both academic and non-academic issues.

I would take this opportunity to acknowledge my professors at KAUST, particularly Dr. Ahmed Sultan Salem, Prof. Tareq-Al-Naffouri, Prof. Marc Genton and Dr. George Turkiyyah for their devotion and encouragement. They have been a source of great inspiration for me. I also acknowledge the support of all my friends at KAUST who made this journey fun and memorable. Special thanks to KAUST for providing me this unique opportunity to enrich myself and to get to know such wonderful people with whom I have established lifelong relationships.

Finally, I would like to thank my parents, whose prayers and encouragement have always been a source of tremendous support for me. To them, I owe all my achievements. My special thanks to my mother for her unconditional love and support in all my matters and I dedicate this thesis to her.

# TABLE OF CONTENTS

**Examination Committee Approval** **2**

**Copyright** **3**

**Abstract** **4**

**Acknowledgements** **6**

**List of Figures** **10**

**List of Tables** **12**

**List of Symbols** **13**

**List of Symbols** **14**

**1 Introduction** **15**

1.1 Vehicular Communication . . . . . 16
1.2 Spectrum Access Methods for Reliable Communication . . . . . 18
1.3 Network Geometry . . . . . 19
1.4 Key Performance Metrics . . . . . 20
1.5 Motivation & Objective . . . . . 21
1.6 Scope & Contribution of the Thesis . . . . . 22
1.7 Organization of Thesis . . . . . 23

**2 Related Work** **25**

2.1 Stochastic Geometry . . . . . 25
2.2 Vehicular Networks . . . . . 26
2.3 Stochastic Geometry Analysis of Vehicular Communication . . . . . 26

**3 Modeling and Analysis of Inter-vehicle Communication in Multi-Lane Highways with saturated transmission buffers** **29**

3.1 Introduction . . . . . 29
3.2 System Model . . . . . 30
3.2.1 Modeling Approaches . . . . . 30
3.2.2 Network Model . . . . . 32
3.2.3 Methodology of Analysis . . . . . 34
3.3 SINR Characterization . . . . . 34
3.3.1 Distance Distribution . . . . . 35
3.4 Performance Analysis . . . . . 36
3.4.1 Same-lane Transmitter . . . . . 37
3.4.2 Cross-Lane Transmitter . . . . . 44
3.5 Numerical Results . . . . . 47
3.5.1 System Parameters and Model Validation . . . . . 47
3.6 Conclusion . . . . . 49

**4 Modeling and Analysis of Inter-vehicle Communication in Multi-Lane Highways with un-saturated transmission buffers 52**
4.1 Introduction . . . . . 52
4.2 System Model . . . . . 53
4.3 Methodology . . . . . 54
4.3.1 Intensity of Concurrent Transmitters . . . . . 55
4.3.2 Iterative Algorithm . . . . . 55
4.4 Numerical Results . . . . . 55
4.5 Conclusion . . . . . 57

**5 Modeling & Analysis of Multi-hop communication in highway VANETs 59**
5.1 Introduction . . . . . 59
5.2 System Model . . . . . 60
5.2.1 Network Model . . . . . 60
5.3 Packet Forwarding Strategies . . . . . 62
5.3.1 Most Forward with Fixed Radius (MFR) . . . . . 62
5.3.2 Nearest with Forward Progress (NFP) . . . . . 62
5.3.3 Random with Forward Progress (RFP) . . . . . 63
5.4 Methodology of Analysis . . . . . 63
5.4.1 SINR Characterization . . . . . 63
5.4.2 Distance Distribution . . . . . 64
5.5 Performance Analysis . . . . . 66
5.5.1 Probability of Transmission Success . . . . . 66

5.5.2 Normalized Average Forward Progress . . . . . 68
5.5.3 Aggregate Packet Progress . . . . . 70
5.6 Simplifying Approximations . . . . . 71
5.7 Numerical Results & Discussion . . . . . 72
5.7.1 System Parameters and Model Validation . . . . . 72
5.7.2 Maximizing Transmission Capacity & Forward Progress . . . . 77
5.8 Conclusion . . . . . 78

**6 Conclusion** **79**

**References** **80**

**Appendices** **86**

# LIST OF FIGURES


3.1 Modeling approaches for multi-lane highway. . . . . 30
3.2 Comparison of models for highway IVC in simulation. . . . . 31
3.3 Multi-lane highway vehicular network. . . . . 31
3.4 Distance of a potential transmitter to a test receiver at the origin. . . . . 35
3.5 Single Lane Highway (N = 1) . . . . . 37
3.6 Multi-lane highway (N = 3), same lane transmitter. . . . . 40
3.7 Mapping of uniformly spaced points on to the line through the origin. . . 41
3.8 Multi-lane highway, cross lane transmitter. . . . . 44
3.9 Model validation. . . . . 47
3.10 Success Probability against Traffic Intensity and Detection Threshold for Multi-Lane Highway. . . . . 50
3.11 Optimizing sensing range of vehicles for different inter-lane distances . . . 51

4.1 Single node queueing system. . . . . 53
4.2 Model validation with unsaturated buffers. . . . . 56
4.3 Success probability for multi-Lane highway (N=11) in sparse traffic with unsaturated buffers. . . . . 57
4.4 Success probability for multi-Lane highway (N=11) in dense traffic with unsaturated buffers. . . . . 58
4.5 Optimizing sensing range of vehicles for different inter-lane distances (unsaturated buffers). . . . . 58

5.1 Message propagation using inter-vehicle communication . . . . . 60
5.2 Multi-lane highway with test transmitter and receiver. . . . . 60
5.3 Model validation for the *MFR* strategy . . . . . 73
5.4 Model validation for the *NFP* strategy . . . . . 73
5.5 Model validation for the *RFP* strategy . . . . . 74
5.6 Normalized average forward progress against sensing range . . . . . 74
5.7 Normalized average forward progress for different traffic intensities . . . . 75
5.8 Maximizing transmission capacity and forward progress . . . . . 75

E.1 Transmitter-Receiver distance for MFR strategy . . . . . 91
F.1 Transmitter-Receiver distance for NFP strategy . . . . . 95

# LIST OF TABLES

1 Table of Acronyms . . . . . 13
2 Table of Notations . . . . . 14

5.1 Simulation Parameters . . . . . 76

# LIST OF ACRONYMS

Table 1: Table of Acronyms

| Notation | Definition |
|---|---|
| ITS | Intelligent transportation systems |
| NHTSA | National highway traffic safety administration |
| VANET | Vehicular adhoc network |
| V2V | vehicle-to-vehicle |
| V2R | vehicle-to-roadside |
| IVC | Inter vehicle communication |
| MAC | Medium access control |
| CSMA | Carrier sense multiple access |
| PPP | Poisson point process |
| MHCPP | Matérn hard core point process |
| MHCPP-II | Matérn hard core point process of type II |
| SINR | Signal to interference plus noise ratio |
| MFR | Most forward with fixed radius |
| NFP | Nearest with forward progress |
| RFP | Random with forward progress |
| APP | Aggregate packet progress |
| SLA | Single lane abstraction |
| 2D | Two dimensional |
| iid | Independent and identically distributed |
| pdf | probability distribution function |
| ccdf | complementary cumulative distribution function |
| LT | Laplace transform |
| BD | Birth death process |
| QoS | Quality of service |
| WAVE | Wireless access in vehicular environment |

# LIST OF SYMBOLS

Table 2: Table of Notations

| Notation | Definition |
|---|---|
| $N$ | Number of traffic lanes in the highway |
| $P$ | Transmission power of each vehicle |
| $d$ | Distance between parallel traffic lanes in a highway |
| $r_0$ | Distance between transmitter and receiver |
| $\Phi_i$ | PPP of vehicles on the $i^{th}$ traffic lane |
| $\tilde{\Phi}_i$ | PPP of simultaneously transmitting vehicles |
| $\lambda_l$ | Intensity of vehicles in each traffic lane |
| $\Lambda$ | Intensity of simultaneously transmitting vehicles in each lane |
| $R_t$ | Transmission Range of each vehicle |
| $R_s$ | Sensing Range of each vehicle |
| $\zeta$ | Ratio of Transmission Range and Sensing Range |
| $\mathcal{N}$ | Contention domain of a test transmitter at the origin |
| $\mathbf{N}$ | Neighbourhood of a test transmitter at the origin |
| $\rho_{th}$ | Sensing threshold |
| $\rho_{min}$ | Receiver Sensitivity |
| $T$ | Signal decoding threshold |
| $\eta$ | Path loss exponent |
| $\kappa$ | Noise floor |
| $\mu$ | $1/\mu$ is the mean of the exponential fading distribution |

# Chapter 1

# Introduction

Wireless Communication is composed of a transmitter, a receiver and a propagation channel. The transmitter sends out a modulated electromagnetic signal which propagates through the channel and reaches the receiver after being corrupted by noise, interference and other channel impairments such as path-loss, fading and shadowing. Path loss is a large scale propagation effect and is dependent on the distance, $r$ between the transmitter and the receiver. Generally, it is considered that path loss $\propto r^{-\eta}$, where $\eta$ is the path loss exponent. Similarly, shadowing is a large scale propagation effect and depends on the obstacles between the transmitter and receiver. Fading, however, is a random phenomena and its effect is modeled by random distributions such as Rayleigh (in the case of multiple scatterers without line of sight component) and Rician distributions (in the case of line of sight component).

The wireless spectrum is divided into several frequency bands, also known as channels. A communication link can be established on each channel independently of other channels without causing interference, provided that the channels are sufficiently separated from each other. Multiple transmissions on a single channel would interfere with each other resulting in distortion of the signal at the receiver. Only the dominant signal can be recovered correctly at the receiver given that its signal-to-noise-plus-interference (SINR) exceeds a particular threshold. A medium access control (MAC) protocol is required for coordinating the spectrum access by multiple users. This will

be further elaborated later in this chapter.

Wireless communication allows us the flexibility to communicate while moving as opposed to wired communication in which communicating nodes have fixed locations. An important application of wireless communication is in vehicular communication where the communicating nodes are highly mobile and create a random network topology.

## 1.1 Vehicular Communication

Vehicular communication is the communication involving vehicles on the road. The ability of a vehicle to communicate with other vehicles and with base stations, can lead to exciting applications for safety, comfort and efficiency of transport.

Recently, there has been a strong focus on improving the efficiency and safety of transportation and this has led to the development of the Intelligent Transportation Systems (ITS). While ITSs cover all forms of transportation, including road, rail, air and water transportation, communication for road networks is of special interest due to its uncoordinated and less controlled nature when compared to the other transportation systems. While planes, trains, and ships are usually driven by highly trained personnel, cars are driven by public varying in their skills, which raises serious safety issues for road transportation. For instance, according to the US census bureau, the US has a round figure of 10 million road accident per year with an average of 1.5 % fatality rate [1]. The US national highway traffic safety administration (NHTSA) reports that an average of 90 death and more than 6000 injuries occur every day, across the US, due to car accidents [2]. Hence, there is a high demand to incorporate an automated and intelligent system to compensate for the human error, which is considered the major cause for accidents. In this context, vehicles can communicate with each other to alert drivers, or even take automated actions, to avoid collisions and

save lives. Vehicular communication can also offer potential gains from an economical perspective. A recent report by *The Economist* estimated the total cost of traffic jams across four countries (US, UK, Germany, and France) to be 200 billion dollars [3].

Existing vehicular safety systems are mainly composed of either light based proximity sensors or radar systems which are limited in detection range and proximity coverage. Wireless communication based vehicular communication systems provide a much larger communication range which allows for more advanced and pro-active safety systems that warn drivers about potential dangers even before they are able to see them. Vehicular adhoc networks (VANETs) [4] can be exploited to improve navigation systems and alleviate traffic jams. That is, to develop real time and context-aware navigation systems that collect real-time traffic information, via the vehicular network, to take appropriate navigation decisions. This will not only save money and time wasted in traffic jams, but also will offer a better user experience via information based vehicular applications. For instance, [5] presented a novel navigation paradigm that adds the achievable data rate and traffic condition to the traditional distance based route selection scheme. To this end, vehicular communication systems are envisioned to be the key enabler for safe and efficient road transportation.

A typical vehicular communication system consists of three different links or modes of operation, namely, Vehicle-to-Vehicle (V2V), Vehicle-to-Roadside (V2R), and Roadside-to-Roadside. The V2V communication, also referred to as Inter-Vehicle Communication (IVC)[6,7] is an enabling technology for a variety of applications such as adaptive traffic control, coordinated braking, emergency messaging, peer-to-peer networking for infotainment services, and automatic toll collection. Further, IVC communication is mandatory in rural places where no roadside base stations are deployed.

In order to have reliable communication and to avoid packet collisions between transmitting vehicles, spectrum access must be coordinated by a set of rules. These

rules are defined in the form of medium access protocols. In the following section, two commonly used spectrum access methods are discussed.

## 1.2 Spectrum Access Methods for Reliable Communication

Medium Access Control (MAC) is used to coordinate sharing of the wireless spectrum by multiple users. Several MAC protocols have been developed for wireless communication such as ALOHA [8] and Carrier Sense Multiple Access (CSMA) [9]. ALOHA protocol does not restrict the transmission of a transmitter and relies on the receipt of the acknowledgement from the receiver. According to the IEEE standard, IVC is coordinated via CSMA MAC protocol. CSMA is a contention based spectrum access technique that is controlled by means of random backoff counters. That is, each transmitter, that intends to transmit a packet, generates a random backoff timer which is decremented if the channel is sensed idle and freezed if the channel is sensed busy. Only transmitters with elapsed backoff timers can transmit. Hence, a transmission is only initiated in an idle channel state to avoid packet collisions. The idle/busy state of the channel is determined by the sensing threshold ($\rho_{th}$), which is a vital design parameter for the CSMA protocol. The sensing threshold is the cut-off power level below which it is assumed that the channel is idle. The effects of $\rho_{th}$ on the system performance will be discussed later in this thesis.

Since the wireless medium is a shared resource, and the transmitted signals decay with the distance in all directions, therefore the location of communicating nodes plays an important part in the MAC protocol. Communicating nodes in close proximity to each other cannot transmit at the same time to avoid interfering with each other. On the other hand, nodes sufficiently separated by each other can transmit simultaneously. The distances between communicating terminals depends on the type

of the network and its objectives. The topic of node locations in the network is discussed in the following section.

## 1.3 Network Geometry

Network geometry deals with the location of wireless communicating nodes in a network. The spatial distribution of nodes determines the interference in the network and hence contributes greatly to the SINR levels at the receiver. The network geometry is affected by the nature of the network for instance sensor networks have a random geometry and nodes can be located anywhere in space. On the other hand, cellular networks have a well planned geometry of base stations. Different from general ad-hoc networks, vehicular networks have their own characteristics (e.g. geographical limitation to roads) that should be incorporated into the modeling framework. The location of moving vehicles on the roads at any instant of time is completely random. The network topology depends on the type of road network. Highways will have a different pattern of vehicles as compared to urban road systems with intersecting roads. In this thesis, I focus on highway vehicular systems which comprises of a set of parallel roads.

The developed analytical paradigm is based on stochastic geometry [10] analysis and point process theory. The Poisson Point Process (PPP), which assumes independent point locations, is the most popular point process used in literature due to its simplicity and tractability. While it is acceptable to assume that the locations of the vehicles are uncorrelated on highways, I cannot assume uncorrelated locations for the subset of concurrent transmitting vehicles due to the CSMA spectrum access. Instead, the Matérn hard core point process type II (MHCPP-II) captures the correlation among the set of simultaneously transmitting vehicles due to the contention based access [11–13]. Starting from the PPP representing the total set of potential

transmitters, the MHCPP-II captures the repulsive behavior between the concurrent transmitters, imposed by the CSMA protocol, via dependent thinning. In the process of dependent thinning, points are given a uniformly distributed mark [0,1] and only the points which have the least mark in their neighbourhood are retained. The uniform mark corresponds to the back-off counter value chosen by each node in the CSMA protocol. Considerable amount of efforts have been invested to characterize CSMA based networks using the MHCPP-II [11–13].

## 1.4 Key Performance Metrics

Stochastic geometry has been the tool of choice in this thesis due to its ability to handle random networks and to characterize interference in such networks. Therefore, the primary quantity of interest is the SINR. The key performance metrics of the system are defined as follows:

- **Probability of Transmission Success:**

  The probability of transmission success is the probability that the SINR at the receiver exceeds a particular decode threshold ($T$). It is defined as $\mathcal{P} = \mathbb{P}[SINR > T]$.

- **Spatial Frequency Reuse Efficiency:**

  The spatial frequency reuse efficiency metric measures how often the same frequency channel is used over the spatial domain. This is directly related to the CSMA sensing threshold ($\rho_{th}$) because a lower threshold would force the same channel to be reused after a greater area and hence a smaller spatial frequency reuse efficiency and vice versa.

- **Transmission Capacity:**

  The transmission capacity is defined as the number of successful transmissions

per unit area. It depends on both the transmission success probability and the total number of transmitters/transmissions at the same time.

There are other metrics that have been used to measure the performance of the network under the multi-hop communication. However they have been defined in the relevant chapter to avoid ambiguity at this stage.

## 1.5 Motivation & Objective

Motivated by the impact of the CSMA sensing threshold on the probability of transmission success and the spatial frequency reuse efficiency in a VANET, the aim of the thesis is to develop an analytical model for IVC in multi-lane highways to study the tradeoffs and to tune the sensing threshold in order to improve system performance.

The sensing threshold of the CSMA MAC imposes a crucial tradeoff between the probability of successful transmission, denoted by $\mathcal{P}$, and the spatial frequency reuse efficiency. A lower sensing threshold enforces larger distances between concurrent transmitters, which decreases interference and increases the transmission success probability, on the expense of degrading the spatial frequency reuse, and vice versa. Hence, the sensing threshold ($\rho_{th}$) should be carefully tuned to balance the tradeoff between the transmission success probability and spatial frequency reuse efficiency.

A good selection for $\rho_{th}$ guarantees an efficient local communication between vehicles. However, several vehicular applications require going beyond the local communication and efficiently disseminate information across the roads via multi-hops. For instance, if there is an accident on a highway, the incident can be immediately reported to the nearest ambulance or emergency center using the multi-hop vehicular network. Also in the case of highway congestion, it is important to disseminate the incident far enough so that other vehicles can take appropriate navigational decisions and change the selected trajectory to alleviate the congested sector. Therefore, pack-

ets need to be efficiently propagated from one hop to another until the destination. There are different message forwarding schemes, that compromise different tradeoffs between message froward progress and per-hop success probability ($\mathcal{P}$), for packet dissemination. In particular, I focus on the most forward with fixed radius (MFR), the nearest with forward progress (NFP), and the random with forward progress (RFP). As it is clear from the protocol names, the MFR favors relaying the packets to the farthest vehicle to maximize the forward progress on the expense of lower per-hop success probability. On the contrary, the NFP favors nearby vehicle relaying to attain a high per-hop transmission success probability on the expense of low forward progress. The RFP achieves a midpoint performance between the MFR and the NFP. It is worth mentioning, as will be shown in the results, that there is an interaction between the sensing threshold and the packet forwarding protocols. For instance, to have an acceptable probability of success, the MFR requires more conservative $\rho_{th}$ due to the large hop distance as compared to the NFP which can sustain an aggressive $\rho_{th}$ due to the smaller hop distance. Therefore, an efficient packet forwarding scheme should balance the tradeoff between the probability of success, forward packet progress, and the spatial frequency reuse efficiency imposed by both the forwarding scheme and the CSMA parameter $\rho_{th}$.

## 1.6 Scope & Contribution of the Thesis

In this thesis, I focus on the IVC aspects in vehicular networks in a multi-lane highway scenario. In the first part of the thesis, local communication is considered under the assumption of saturated traffic. This implies that all the network nodes will have packets to transmit at all times. This assumption is subsequently relaxed using a queueing theory model and the effect of unsaturated transmission buffers is incorporated into the analysis. In the second part of the thesis, the multi-hop vehicular

communication is considered. Different transmission strategies available to transmitting vehicles are described and their effect on the efficiency of packet dissemination is discussed. A comparison is made between the transmission strategies using a unified performance metric and the best transmission strategy is identified. The main contributions of this thesis are:

1. To develop a novel tractable framework to model inter-vehicle communication in a multi-lane highway network based on stochastic geometry analysis.

2. To compare between various abstraction models used for highway vehicular networks and show that the widely used line abstraction model does not accurately model the probability of transmission success for wide highways.

3. To study different message dissemination strategies via multi-hop communication in CSMA based IVC and compare their performance under different traffic conditions.

4. To define the aggregate packet progress (APP) metric which captures the trade-off between success probability, forward progress, and spatial frequency reuse.

5. To show that there exists an optimal sensing threshold of the CSMA protocol that maximizes the APP.

## 1.7 Organization of Thesis

The thesis is organized as follows: In chapter 2, I present the existing work in literature related to the thesis. Chapter 3, develops the foundation of the proposed analytical framework for single hop communication under the case of saturated transmission buffers. In Chapter 4, the analysis and results are provided for the case of unsaturated transmission buffers. In Chapter 5, the model is extended to multi-

hop communication and different packet forwarding strategies are studied. Finally Chapter 6 concludes the thesis and provides insights on future directions.

# Chapter 2

# Related Work

Vehicular communication in VANETs has been a hot research area in recent years. Different from general ad-hoc networks, vehicular networks have their own characteristics (e.g., geographical limitation to roads) that should be incorporated into the modeling framework. Considerable efforts have been put in the design of these networks. Stochastic geometry has long been used in the design and analysis of cellular and adhoc networks. Interestingly, stochastic geometry has also been used in literature to model vehicular networks. In this chapter, I divide the related work into three sections. The first section reviews the work done using stochastic geometry in the design of wireless networks. The second section deals with the literature related to vehicular communication. Finally, the third section mentions existing works which have used stochastic geometry to model vehicular networks.

## 2.1 Stochastic Geometry

Stochastic geometry [14–19] is a powerful mathematical and statistical tool and it has been used extensively to model large scale and adhoc networks. It provides spatial averages i.e. average over all network realizations of quantities such as SINR, Outage/Coverage probability and Data Rate etc... It not only captures the random network topologies but also provides tractable analytical models for communication

networks. It has been particularly useful in modeling networks with random channel access such as ALOHA [20–24] and CSMA [11, 13, 25–27]. Stochastic geometry has also been used in modeling single-tier and multi-tier cellular networks [28–31].

## 2.2 Vehicular Networks

Vehicular networks are a special case of mobile adhoc networks. IEEE has established a standard for vehicular communication known as wireless access in vehicular environment (WAVE) [32, 32] which is based on the IEEE 802.11p protocol. Several works are available on the modeling and analysis of vehicular communication. Some of them are based on simulation [33–35] studies while others provide analytical models [36, 37]. A large proportion of the literature on vehicular networks that provide analytical models ignores the relative mobility effects between vehicles and consider . However mobility models have been developed and are provided in [38, 39]. Several analytical models have been based on stochastic geometry analysis which is discussed in the following section.

## 2.3 Stochastic Geometry Analysis of Vehicular Communication

Stochastic geometry has been used in literature to develop analytical models for vehicular networks. For instance, the authors in [36] and [37] developed an analytical model for VANETs to maximize the throughput, however, the presented models are based on slotted ALOHA protocol which does not aptly capture the effect of CSMA spectrum coordination in vehicular networks. VANET models with CSMA spectrum access are studied in [40–43] but are either based on simulation studies or are approximated by ALOHA. In [40], a Markovian approach is used to compute the maximum

possible spatial reuse in a VANET using the single lane abstraction (SLA). SLA abstracts multi-lanes to a single lane with the sum of traffic intensities. The authors in [41] analyzed the performance of the IEEE 802.11p version of the CSMA protocol which is defined for vehicular communication. The 802.11p is discriminated from the traditional CSMA protocol by the discrete backoff timer values, which is intended to decrease the time required for spectrum access. However, discrete backoff timers arise a possibility of having collisions within the sensing range due to backoff ties among neighboring vehicles. In fact, [41] showed that, due to the backoff timer ties problem, the performance of the IEEE 802.11p approaches the performance of the ALOHA protocol in high node densities and therefore the analysis is provided for the ALOHA regime. To overcome the collision problem imposed by the discrete backoff timer of the 802.11p, several papers (e.g. [44] and [45]) proposed adaptive contention window size techniques. IEEE 802.11p is also studied in [43], however, the analysis relies on the SLA model and is limited to the local vehicular communication. The authors in [42] study the performance of local vehicular communication using IEEE 802.11p however their studies are based on simulations.

The packet forwarding protocols for multi-hop communication used in this thesis have been studied for ALOHA based adhoc networks [21]. However these models were developed using planar 2D PPPs for uncoordinated spectrum access networks. In contrast, this thesis evaluates the performance of the packet forwarding protocols in a restricted multi-highway setting with CSMA coordinated spectrum access protocol. It is worth noting that in ALOHA networks, NFP outperforms the MFR due to the high interference level in the network. On the contrary, the results show the outperformance of the MFR, thanks for the CSMA spectrum access coordination scheme.

Different from the studies presented in the literature, in this thesis, the performance of CSMA coordinated multi-hop communication in multi-lane highway vehic-

ular networks is investigated. The main focus of the thesis is to study the tradeoff imposed by the CSMA sensing threshold on the packet transmission success probability, forward packet progress and the spatial frequency reuse efficiency. Note that the contention domain collision problem of the 802.11p is out of the scope of the thesis. The proposed analysis does not rely on the SLA model and instead, captures the effect of the number of traffic lanes and the inter-lane separation.

# Chapter 3

# Modeling and Analysis of Inter-vehicle Communication in Multi-Lane Highways with saturated transmission buffers

## 3.1 Introduction

In this chapter, a modeling framework is developed to capture the interactions of communicating vehicles in a general multi-lane highway setup. The main approaches that can be used to model highway VANETs are discussed. The approach used in this thesis and the associated network model is described along with stating the underlying assumptions. The analysis is presented in a step by step manner beginning from a single lane highway network to the general case. Finally the numerical results are provided along with the derived insights from the model. It is important to note that in this chapter, the analysis assumes saturated transmission buffers i.e. the transmission buffer at each vehicle always has a packet to be transmitted. This assumption will be relaxed in chapter 4.

## 3.2 System Model

### 3.2.1 Modeling Approaches

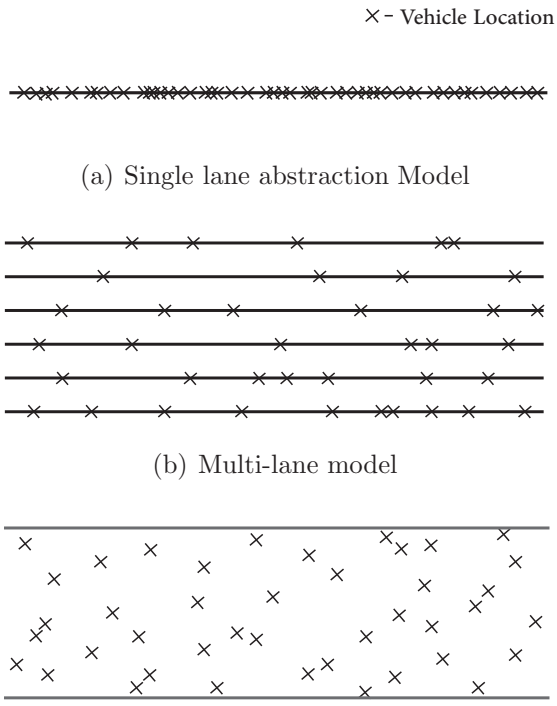


(a) Single lane abstraction Model

(b) Multi-lane model

(c) 2-D PPP model

Figure 3.1: Modeling approaches for multi-lane highway.

There are three main approaches to model vehicles on a multi-lane highway as illustrated in Fig. 3.1. The first approach, which is widely used in literature, is known as the Single Lane Abstraction (SLA) model or simply the line abstraction model shown in Fig. 3.1(a) in which all the traffic lanes are merged into a single lane with the aggregated traffic intensity. This greatly simplifies the analysis. However, it has been shown in this chapter that the line abstraction model cannot accurately characterize the performance of highway vehicular networks when the highway is significantly wide and under high traffic intensity. The second approach is to consider that the traffic is restricted into individual lanes separated by a fixed inter-lane distance. This is

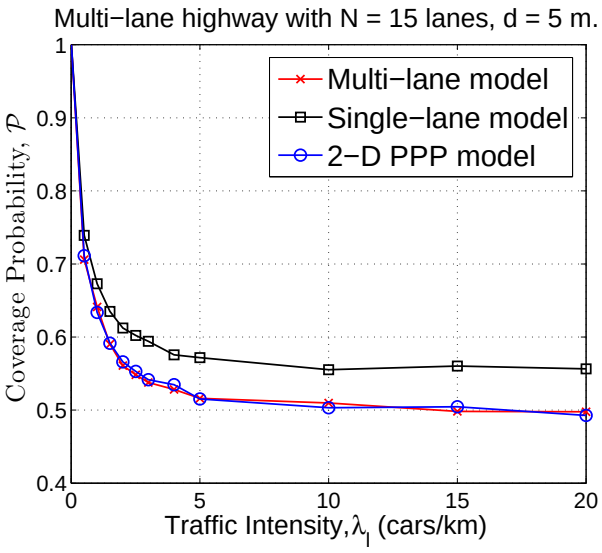


Figure 3.2: Comparison of models for highway IVC in simulation.

illustrated in Fig. 3.1(b) and will be the approach used in this thesis. The third approach as illustrated in Fig. 3.1(c) models the highway traffic using a 2-D PPP restricted to the area covered by the highway. This approach gives one more degree of freedom on the location of the vehicles. However it is not tractable. A simulation study comparing the results of the three approaches for a multi-lane highway with 15 traffic lanes and an inter-lane separation of 5 m (see Fig. 3.2) shows that the multi-lane approach and the 2-D PPP approach give approximately the same results while the SLA model overestimates the probability of successful transmission. Therefore, in this thesis, a tractable framework is developed using the multi-lane model.

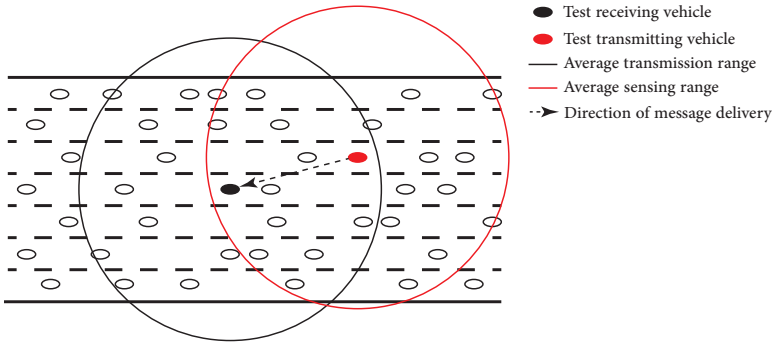


Figure 3.3: Multi-lane highway vehicular network.

### 3.2.2 Network Model

Lets consider a highway VANET in which the traffic lanes are modeled by parallel lines existing in the $\mathbb{R}^2$ plane and separated by fixed distances $d$. On each traffic lane, the vehicles are modeled via an independent homogenous 1-D Poisson Point Process (PPP), $\Phi_i = \{v_{ij}; j = 0, 1, 2, ...\}$, where $i = 1, \ldots, N$, is the lane index and $j$ is poisson distributed with mean $\lambda_l$ cars/km. $v_{ij}$ represents the location of the $j^{th}$ vehicle on the $i^{th}$ traffic lane. Since the speed of packet transmission, including the delays due to back-off, is much faster than the speed of vehicles, it is reasonable to assume that the locations of the vehicles are fixed during contention and packet transmission. This is formally stated as:

**Assumption 1.** *It is assumed that the vehicles are stationary during the packet transmission and the relative mobility effects can be ignored in the analysis.*

**Remark 1.** *According to [46], the maximum average wait time before transmission is estimated to be* 264 $\mu s$ *and the total packet delivery time is in the order of milliseconds. Therefore on a* 80 *km/h highway, a vehicle will be displaced by much less than* 1 $m$ *during a single transmission. This makes it reasonable to ignore the effect of mobility on a single link performance.*

A snapshot of the system model is provided in Fig. 3.3. It is assumed that all vehicles transmit with a fixed transmit power of $P$ and that each vehicle always has a packet to transmit (i.e. the transmission buffers are saturated). The signal power decays with the distance $r$ according to the power law $r^{-\eta}$, where $\eta > 1$ is path-loss exponent. The channel between vehicles experiences independent Rayleigh fading in which the channel power gain denoted by $h$ has an exponential distribution with mean $\mu^{-1}$. Thus the received power at a typical vehicle from a transmitting vehicle separated by a distance $r$ is given by $Phr^{-\eta}$. The transmit power $P$, the path-loss attenuation, and the receiver sensitivity $\rho_{min}$ determines the average transmission

range of the vehicles as $R_t = \left(\frac{P}{\mu\rho_{min}}\right)^{\frac{1}{\eta}} \Gamma(1+\frac{1}{\eta})$. I consider a signal capture model in which the received signal can be decoded if and only if the signal-to-interference-plus-noise-ratio (SINR) at the receiver is above a certain threshold $T$.

All vehicles contend for channel access according to the CSMA protocol. For the CSMA contention process, I have the following assumption:

**Assumption 2.** *The framework assumes an intact CSMA protocol performance in which the probability of back-off timer ties between vehicles in the same contention domain is negligible.*

**Remark 2.** *The basic operation of the IEEE 802.11p is similar to the conventional operation of the CSMA protocol except for the higher collision probability within the contention domain. For this reason, several efforts has been invested to adapt the contention window (i.e., backoff timer size) to alleviate this problem [44, 45]. Since the framework proposed in this thesis focuses on the spatial domain uncertainties and abstracts time dynamics, I can safely assume that the contention domain collision problem is solved by one of the techniques proposed in the literature (e.g., [44, 45]).*

All vehicles use an equal spectrum sensing threshold $\rho_{th}$, which is the main design parameter in this thesis. The sensing threshold $\rho_{th}$ determines the neighborhood[1] of the contending vehicles. Due to the CSMA contention, two neighboring vehicles cannot simultaneously transmit. The neighborhood of a typical vehicle $v_i$ can be expressed as $\mathcal{N}_{v_{ij}} = \left\{v_{mn} : Ph \left\|v_{ij} - v_{mn}\right\|^{-\eta} \geq \rho_{th}, \forall m, n\right\}$, where $\|.\|$ is the Euclidean norm. From the reciprocity of the wireless channel, if $v_{ij}$ is a neighbor for $v_{mn}$, then the converse is also true. Since all the neighborhood sets are statistically equivalent, hereafter, I will drop the index $v_{ij}$ (i.e., use $\mathcal{N}$ to denote the neighborhood set of a typical vehicle) for notational convenience.

[1] Vehicles within the sensing range of each other are referred to as neighboring vehicles

### 3.2.3 Methodology of Analysis

The objective of the analysis is to study the tradeoff between the probability of success and the spatial frequency reuse efficiency imposed by the CSMA parameter $\rho_{th}$. In the following sections, I describe the procedure for evaluating the probability of transmission success. With slight loss in generality, the analysis is conducted at the *central lane* of a symmetric N-lane highway. That is, a test node will always be located at the central lane, however it can interact (i.e. transmit and/or receive) from other vehicles on other lanes. It is straightforward to modify the proposed framework for different lanes or for an asymmetric N-lane highway.

## 3.3 SINR Characterization

A transmission is considered successful (i.e. correctly decoded by the receiver) if SINR is above a predefined threshold. The SINR can be written as:

$$\text{SINR} = \frac{P h_o r_o^{-\eta}}{\kappa + \underbrace{\sum_{i=1}^{N} \sum_{v_{ij} \in \tilde{\Phi}_i \setminus v_0} P h_{ij} \left\| v_{ij} \right\|^{-\eta}}_{I_{agg}}}, \tag{3.1}$$

where $\tilde{\Phi}_i \setminus v_0$ is the set containing the simultaneously transmitting vehicles on the $i^{th}$ lane excluding the intended transmitter $v_o$. Note that $\tilde{\Phi}_i \subseteq \Phi_i$ due to the CSMA protocol. $h_o$ and $h_{ij}$ are independent and identically distributed (i.i.d.) random variables representing, respectively, the channel fading between the test receiving vehicle, intended transmitting vehicle, and the $ij^{th}$ interfering vehicle, $r_o$ is a random variable representing the distance between the test receiving vehicle and the intended transmitting vehicle, $v_{ij} \in \mathbb{R}^2$ is the location of the $ij^{th}$ interfering vehicle, and $\kappa$ is

the noise variance. The transmission success probability can be expressed as:

$$\begin{aligned}\mathcal{P} &= \mathbb{P}[SINR > T] \\ &= \int_r \mathbb{P}[\frac{Ph_o r^{-\eta}}{\kappa + I_{agg}} > T] f_{r_o}(r) dr \\ &\overset{(a)}{=} \int_r \exp\left\{-\frac{T\mu\kappa r^\eta}{P}\right\} \exp\left\{-\frac{T\mu I_{agg} r^\eta}{P}\right\} f_{r_o}(r) dr \\ &\overset{(b)}{=} \int_r \exp\left\{-\frac{T\mu\kappa r^\eta}{P}\right\} \mathcal{L}_{I_{agg}}\left(\frac{T\mu r^\eta}{P}\right) f_{r_o}(r) dr, \end{aligned} \tag{3.2}$$

where $\mathcal{L}(.)$ is the Laplace transform (LT) of the probability distribution function (*pdf*) of $I_{agg}$, $(a)$ follows from the exponential distribution of $h_o$, and $(b)$ follows from the definition of the LT. From (3.2) it is clear that I have to obtain the LT of the aggregate interference as well as the *pdf* of $r_o$ in order to derive the success probability.

### 3.3.1 Distance Distribution

The distance distribution between the transmitter and receiver i.e. the *pdf* of $r_o$ is given by the following lemma:

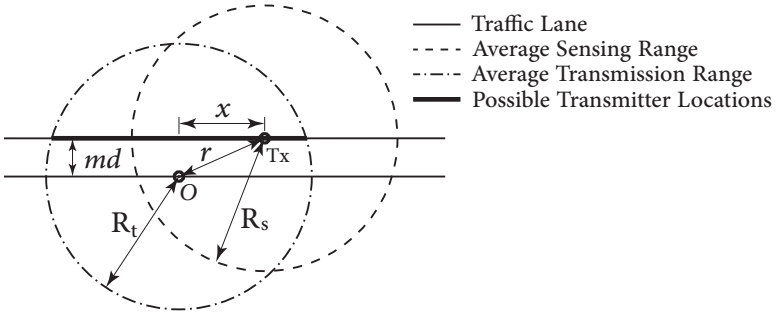


Figure 3.4: Distance of a potential transmitter to a test receiver at the origin.

**Lemma 1.** *For a multi-lane highway, depicted in Fig. 3.4, with an inter-lane distance of $d$, the distance between the origin and a generic vehicle on the $m^{th}$ lane within a circle of radius $R_t$ centered at the origin such that $m = 0, 1, 2, ..\lfloor \frac{R_t}{d} \rfloor$, where $\lfloor . \rfloor$ is the*

*floor function, is distributed as follows:*

$$f_{r_o}(r) = \frac{r}{\sqrt{(R_t^2 - (md)^2)(r^2 - (md)^2)}}; \qquad md \leq r \leq R_t$$
$$\stackrel{m=0}{=} \frac{1}{R_t} \tag{3.3}$$

*Proof.* See **Appendix A** □

In the following sections, I consider two main scenarios to characterize the performance in a general highway setup namely, the same-lane transmitter and cross-lane transmitter. For each of the considered cases, I will characterize the intensity of concurrent transmitting vehicles and the success probability.

## 3.4 Performance Analysis

Due to the contention based channel access, at a given time instant, only the set of vehicles who won the contention (i.e., have elapsed back-off counter) can transmit. Hence, the aggregate interference comes from a set $\tilde{\Phi}_i \subseteq \Phi_i$. The set of concurrent transmitting vehicles can be modeled via the MHCPP-II to capture the repulsive behavior imposed by the CSMA protocol. Note that, due to random channel fading, the notion of distance in the model is based on the channel power gains (i.e., $hr^{-\eta}$) rather than the Euclidean distance $r$. Starting form the complete set of vehicles $\Phi_i$, the MHCPP-II marks $\Phi_i$ with a uniform mark [0,1] and retains only the points with the lowest mark within their neighborhood, where the uniform mark corresponds to the back-off counter value. In other words, the MHCPP-II retains one point within each contention domain. According to [11–13] the intensity of $\tilde{\Phi}_i$ is given by:

$$\Lambda = \lambda_l \frac{1 - e^{-\mathbb{E}[|\mathcal{N}|]}}{\mathbb{E}\left[|\mathcal{N}|\right]}, \tag{3.4}$$

where $|.|$ is the set cardinality.

For the sake of simple presentation, I begin by modeling the simplest case highway setup, then I generalize the model step-by-step until I reach the most general symmetric highway setup. In a highway setup, for a test receiver located on the central lane, the transmitter can either lie on the same lane as the receiver or on a different lane. In each of the presented cases, I first derive the expected cardinality of the neighborhood set of a typical vehicle to characterize the intensity of concurrent transmitting vehicles as in (3.4). Then, I derive the LT of the aggregate interference to characterize the success probability as in (3.2).

### 3.4.1 Same-lane Transmitter

#### Single Lane Highway

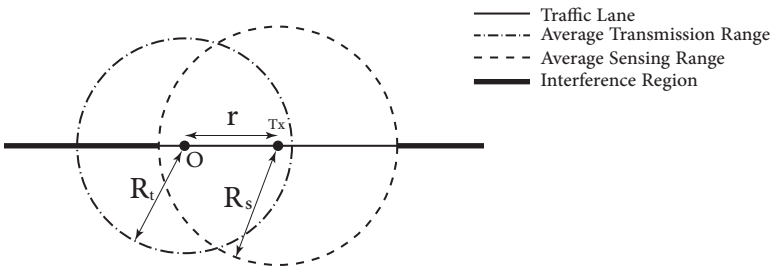


Figure 3.5: Single Lane Highway (N = 1)

I start with the simplest case in which the vehicles exist on a single lane highway as shown in Fig.3.5. In this case, the neighborhood set average cardinality can be characterized via the following lemma.

**Lemma 2.** *In a single-lane highway with Rayleigh fading and CSMA threshold of $\rho_{th}$, the average number of neighbors for a generic vehicle is given by :*

$$\mathbb{E}\left[|\mathcal{N}|\right] = \lambda_l \left(\frac{P}{\mu\rho_{th}}\right)^{\frac{1}{\eta}} \Gamma\left(\frac{1}{\eta}+1\right) = \lambda_l R_s. \tag{3.5}$$

*Proof.* See **Appendix B** □

**Lemma 2** implies that the average contention domain length on each side of a transmitter is given by $\left(\frac{P}{\mu\rho_{th}}\right)^{\frac{1}{\eta}}\Gamma\left(\frac{1}{\eta}+1\right)$, which I denote as $R_s$. It is worth mentioning that the MHCPP-II considers $2R_S$ in the calculation of $\mathbb{E}\left[|\mathcal{N}|\right]$ to account for the contention domain at both sides of each transmitter. Note that, by definition, the MHCPP-II underestimates the intensity $\Lambda$ due to the role of unselected points (see [13] for details). However, due to the natural order of points in 1-D lines, the underestimation problem of the MHCPP-II can be directly related to the contention domain calculations (i.e., $\mathbb{E}\left[|\mathcal{N}|\right]$). I argue that considering the contention domain on both sides of the transmitters, along with retaining one transmitter per contention domain, results in underestimating $\Lambda$ for the following two reasons; i) starting from a retained transmitter and moving in each direction along the line, the first transmitter after a void distance of $R_s$ will contend only with the nodes in the next $R_s$ distance; ii) the MHCPP-II saturates at the intensity of $\frac{1}{2R_s}$ which can be considered as a loose packing density. This is because if $R_s$ is the void region on each side of the transmitters, the intensity of concurrent transmitters should saturate at $\frac{1}{R_s}$. Therefore, throughout this thesis, the proposed contention domain length is $R_s$ as opposed to $2R_s$ used by the MHCPP-II. I show that by using the simple approximation of the contention domain length, the underestimation problem in the 1-D case can be effectively mitigated.

Since the CSMA protocol allows a single transmission per contention domain, the average contention domain length reflects the spatial frequency reuse efficiency. Hence, **Lemma 2** clearly shows the relation between the spatial frequency reuse efficiency with the CSMA design parameter $\rho_{th}$ as well as the network parameters $\eta$, $P$, and $\mu$.

To see the positive effect of $\rho_{th}$ I have to find the LT of the aggregate interference to compute the success probability via (3.2). Note that the interference is coming from the set $\tilde{\Phi}_i$ which constitutes a MHCPP. Finding the LT of interference associated with

a MHCPP is an open problem because there is no known expressions of the probability generating functional for the MHCPP. Therefore, only approximate expressions for the LT are obtained by approximating the MHCPP with an equi-dense PPP. This is formally stated as:

**Assumption 3.** *It is assumed that the interfering set of vehicles $\tilde{\Phi}_i$ constitutes a PPP with intensity $\Lambda$ existing outside the average interference protection imposed by the CSMA protocol as shown in Fig. 3.5. The PPP assumption has proven to be accurate if the intensity $\Lambda$ and interference boundaries are carefully calculated [11–13].*

Following Assumption 3, the success probability is given via the following theorem.

**Theorem 1.** *In a single-lane highway with Rayleigh fading with mean $\mu$ and CSMA threshold of $\rho_{th}$, the probability of transmission success can be expressed as:*

$$\mathcal{P} = \frac{1}{R_t}\int_0^{R_t} e^{-\frac{\mu T r^{\eta}\kappa}{P}} \exp\left(-\int_{\psi\in R^1}\left(\frac{\Lambda}{1+(\frac{\gamma}{rT^{1/\eta}})^{\eta}}\right)d\gamma\right)dr,$$
$$\stackrel{\eta=2}{=} \frac{1}{R_t}\int_0^{R_t} e^{-\frac{\mu T r^2\kappa}{P}} e^{-\Lambda\sqrt{T}r\left(\arctan\frac{\sqrt{T}r}{R_s+r}-\arctan\frac{\sqrt{T}r}{R_s-r}\right)}dr. \tag{3.6}$$

*Note that $\psi$ represents the interference region and from Fig. 3.5, it is clear that the limits of integration are from $R_s + r$ to $\infty$ and from $-\infty$ to $R_s - r$.*

*Proof.* See **Appendix C** □

As will be shown in the results, the success probability is a decreasing function in $\Lambda$, and hence, an increasing function in $\rho_{th}$.

### Multi-lane Highway

Now I extend the previous analysis to the case of an $N$-lane highway where the transmitter and receiver are in the central lane, as depicted in Fig.3.6 for $N = 3$. The

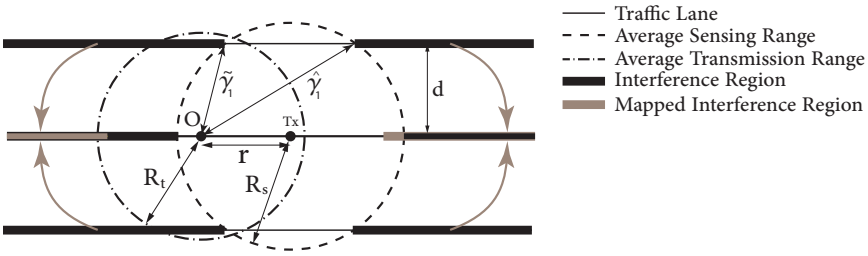


Figure 3.6: Multi-lane highway (N = 3), same lane transmitter.

neighborhood set cardinality of the transmitter in this case is given by the following lemma:

**Lemma 3.** *In an $N$-lane highway with the transmitter in the same lane as the test receiver, the average number of neighbors for a generic vehicle is given by*

$$\mathbb{E}\left[|\mathcal{N}|\right] = \lambda_l \left( R_s + 2 \sum_{i=1}^{(N-1)/2} \sqrt{R_s^2 - (id)^2} \right). \tag{3.7}$$

*Proof.* The proof follows directly from **Lemma 2** and Pythagoras Theorem. □

The multi-lane model illustrated in Fig. 3.6 is complicated and tricky to handle. I propose a three step process to deal with the interference in the multi-lane model. The first step is to identify concurrent transmitters via dependent thinning of the set of parallel PPPs to form a set of MHCPPs. I then approximate the MHCPP on each traffic lane with an equi-dense PPP. Finally I project the homogeneous PPPs on all the traffic lanes to nonhomogeneous PPPs on a single lane via a transformation of intensity. I will use an analogy to calculate the intensity after projection and the boundaries of the PPP as shown in Fig. 3.6 and Fig. 3.7. Consider a set of uniformly spaced points on a line parallel to the line passing through the origin, also referred to as the central lane. From the perspective of the origin, the uniformly spaced points can be mapped to the central lane such that the distance from the origin to the points remains the same. It can be observed clearly from Fig. 3.7 that the points experience a compression which is a function of the distance $\gamma$ from the corresponding point and

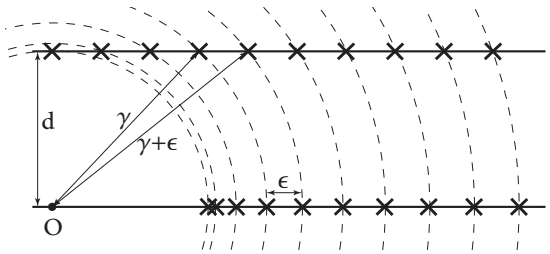


Figure 3.7: Mapping of uniformly spaced points on to the line through the origin.

the origin. The compression factor for the multi-lane scenario is given as follows:

$$c(\gamma, i) = \frac{1}{\sqrt{\gamma^2 + 2\sqrt{\gamma^2 - (id)^2} + 1} - \gamma} \tag{3.8}$$

where $i$ corresponds to the $i^{th}$ traffic lane away from the central lane. I can apply this principle while mapping the homogeneous poisson distributed vehicles to the central lane. Since the compression is non-linear in $\gamma$, so a non-homogeneous PPP is obtained after the mapping operation. Therefore the intensity of the PPP used to model concurrent transmitting vehicles is given by the following lemma.

**Lemma 4.** *The intensity of the PPP of concurrent transmitting vehicles on the $i^{th}$ traffic lane, mapped to the central lane on a multi-lane highway is given by:*

$$\tilde{\Lambda}(\gamma, i) = c(\gamma, i)\Lambda \tag{3.9}$$

Note that $c(\gamma, 0) = 1$ and hence $\tilde{\Lambda}(\gamma, 0) = \Lambda$ i.e. the intensity of the PPP on the central lane remains unchanged under the mapping. It is worth pointing out that the intensity calculation in (3.9) accounts for the contention between vehicles on different lanes. This is because the expression for $\Lambda$ given in (3.4) contains the contention domain size $\mathbb{E}[\mathcal{N}]$ that includes vehicles in all lanes' sections covered by the sensing range as shown in Fig. 3.6. Using this methodology, the framework used in the single lane model can be extended to the multi-lane case. The LT of the aggregate interference for the multi-lane highway is, therefore given by the following lemma:

**Lemma 5.** *The Laplace transform of the aggregate interference observed from a test receiver placed at the origin in a multi-lane highway setup can be expressed as:*

$$\mathcal{L}_{I_{agg}}(s) = \prod_{i=1}^{N} \exp\left( - \int_{\psi_i \in R^1} \left( \frac{\tilde{\Lambda}(\gamma_i, i) P s \gamma_i^{-\eta}}{\mu + P s \gamma_i^{-\eta}} \right) d\gamma_i \right), \tag{3.10}$$

*where $\psi_i$ is the interference region on the $i^{th}$ traffic lane as illustrated in Fig. 3.6.*

*Proof.* See **Appendix D**. □

Using Lemma 5, the probability of transmission success can be evaluated as follows:

**Theorem 2.** *The probability of transmission success in an $N$-lane highway at a test receiver with same lane transmitter is given as follows:*

$$\mathcal{P} = \frac{1}{R_t} \int_0^{R_t} e^{-\frac{\mu T r^{\eta} \kappa}{P}} \prod_{i=-\frac{N-1}{2}}^{\frac{N-1}{2}} \exp\left( - \int_{\psi_i \in R^1} \left( \frac{\tilde{\Lambda}(\gamma_i, i)}{1 + (\frac{\gamma_i}{r T^{1/\eta}})^{\eta}} \right) d\gamma_i \right) dr, \tag{3.11}$$

*where $\psi_i$ is the interference region on the $i^{th}$ traffic lane. Thus the limits of integration are from $\hat{\gamma}_i$ to $\infty$ and from $-\infty$ to $\tilde{\gamma}_i$. The parameters $\hat{\gamma}_i$ and $\tilde{\gamma}_i$ can be expressed as follows:*

$$\hat{\gamma}_i = \mathbb{1}_{\{id \le R_s\}} \sqrt{r^2 + R_s^2 + 2r\sqrt{R_s^2 - (id)^2}} + \mathbb{1}_{\{id > R_s\}}(id),$$
$$\tilde{\gamma}_i = \mathbb{1}_{\{id \le R_s\}} \sqrt{r^2 + R_s^2 - 2r\sqrt{R_s^2 - (id)^2}} + \mathbb{1}_{\{id > R_s\}}(id), \qquad i = 0, 1, \ldots, \frac{N-1}{2}.$$

*and $\mathbb{1}_{\{.\}}$ is the indicator function.*

*Proof.* See **Appendix D**. □

The exact analytical evaluation of the expression in (3.11) for the multi-lane case is not possible. Note that the intractability comes from the fact that the projection of interferers leads to a non-homogeneous PPP with a complicated distance dependent

factor $c(\gamma, i)$. Therefore, for tractability, I suggest two approximations to the success probability. The first is an aggressive interference approximation in which I assume that $\tilde{\Lambda}(\gamma, i) = \sup_{\gamma}(c(\gamma, i))\Lambda$. The second is a conservative interference approximation in which I assume that $\tilde{\Lambda}(\gamma, i) = \Lambda$. That is, the aggressive approximation neglects the intensity decay with the distance from the receiver and the conservative approximation neglects the non-uniform compression effect on the intensity of interferers due to projection. Exploiting these approximations, a single integral expression for the success probability can be obtained.

**Corollary 1.** *The aggressive interference approximation of the probability of transmission success in a multi-lane highways is given by:*

$$\mathcal{P} \approx \frac{1}{R_t}\int_0^{R_t} e^{-\frac{\mu T r^{\eta_\kappa}}{P}} \prod_{i=-\frac{N-1}{2}}^{\frac{N-1}{2}} \exp\left(-\sup_{\gamma}(c(\gamma,i))\Lambda \int_{\psi_i \in R^1} \left(\frac{1}{1+(\frac{\gamma_i}{rT^{1/\eta}})^{\eta}}\right) d\gamma_i\right) dr,$$

$$\stackrel{(\eta=2)}{=} \frac{1}{R_t}\int_0^{R_t} e^{-\frac{\mu T r^2 \kappa}{P}} \prod_{i=-\frac{N-1}{2}}^{\frac{N-1}{2}} e^{-\tilde{\Lambda}(\hat{\gamma}_i,i)\sqrt{T}r \arctan\frac{\sqrt{T}r}{\hat{\gamma}_i} - \tilde{\Lambda}(\tilde{\gamma}_i,i)\sqrt{T}r \arctan\frac{\sqrt{T}r}{\tilde{\gamma}_i}} dr \qquad (3.12)$$

*where $\psi_i$,$\hat{\gamma}_i$ and $\tilde{\gamma}_i$ are given in* Theorem 2.

Similarly, I can obtain the conservative interference approximation for the success probability by using $\tilde{\Lambda}(\gamma, i) = \Lambda$.

**Corollary 2.** *The conservative interference approximation of the probability of transmission success in a multi-lane highways is given by:*

$$\mathcal{P} \approx \frac{1}{R_t}\int_0^{R_t} e^{-\frac{\mu T r^{\eta_\kappa}}{P}} \prod_{i=-\frac{N-1}{2}}^{\frac{N-1}{2}} \exp\left(-\Lambda \int_{\psi_i \in R^1} \left(\frac{1}{1+(\frac{\gamma_i}{rT^{1/\eta}})^{\eta}}\right) d\gamma_i\right) dr,$$

$$\stackrel{(\eta=2)}{=} \frac{1}{R_t}\int_0^{R_t} e^{-\frac{\mu T r^2 \kappa}{P}} \prod_{i=-\frac{N-1}{2}}^{\frac{N-1}{2}} e^{-\Lambda\sqrt{T}r \arctan\frac{\sqrt{T}r}{\hat{\gamma}_i} - \Lambda\sqrt{T}r \arctan\frac{\sqrt{T}r}{\tilde{\gamma}_i}} dr \qquad (3.13)$$

*where $\psi_i$,$\hat{\gamma}_i$ and $\tilde{\gamma}_i$ are given in* Theorem 2.

### 3.4.2 Cross-Lane Transmitter

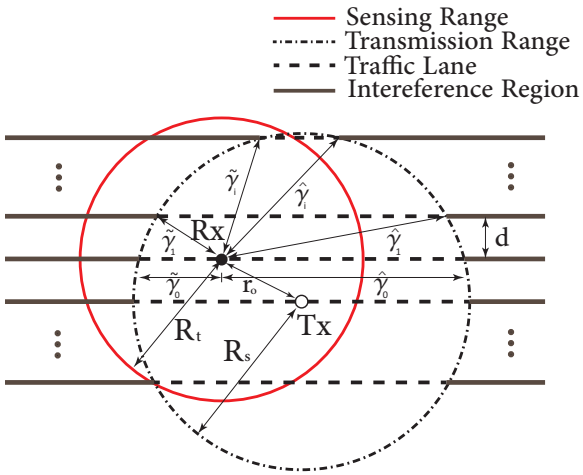


Figure 3.8: Multi-lane highway, cross lane transmitter.

Now I extend the previous analysis to the general case of an $N$-lane highway where the transmitter can be located $m$ lanes away from the central lane where $m = 0, 1, \ldots, \lfloor \frac{R}{d} \rfloor$. This is illustrated in Fig.3.8. The neighbourhood set cardinality of the transmitter in the general case is given by the following lemma:

**Lemma 6.** *In an $N$-lane highway with the transmitter $m$ lanes away from the test receiver, the average number of neighbors for the transmitter is given by*

$$\mathbb{E}\left[|\mathcal{N}|\right] = \lambda_l \left( R_s + \sum_{n=-min\left(\frac{N-1}{2}, \lfloor \frac{R_s}{d} \rfloor\right)}^{min\left(\frac{N-1}{2}, \lfloor \frac{R_s}{d} \rfloor\right)} \sqrt{R_s^2 - ((n-m)d)^2} \right) \tag{3.14}$$

*Proof.* The proof is similar to **Lemma 2** with appropriate limits of the neighborhood domain. □

The probability of transmission success in the general case is then given by the following theorem.

**Theorem 3.** *The probability of transmission success in an $N$-lane highway at a test receiver located at the origin with the transmitter located $m$ lanes away from the central*

*lane is given as follows:*

$$\mathcal{P} = \frac{1}{\sqrt{R_t^2 - (md)^2}} \int_{md}^{R_t} \frac{r}{\sqrt{r^2 - (md)^2}} e^{-\frac{\mu T r^{\eta} \kappa}{P}} \prod_{i=-\frac{N-1}{2}}^{\frac{N-1}{2}} \exp\left( - \int_{\psi_i \in R^1} \left( \frac{\tilde{\Lambda}(\gamma_i, i)}{1 + (\frac{\gamma_i}{rT^{1/\eta}})^{\eta}} \right) d\gamma_i \right) dr, \tag{3.15}$$

*where $\psi_i$ is the interference region on the $i^{th}$ traffic lane as illustrated in Fig. 3.8. Thus the limits of integration are from $\hat{\gamma}_i$ to $\infty$ and from $-\infty$ to $\tilde{\gamma}_i$. The parameters $\hat{\gamma}_i$ and $\tilde{\gamma}_i$ can be expressed as follows:*

$$\begin{aligned}
\hat{\gamma}_i =& \mathbb{1}_{\{|i-m|d<R_s\}} \sqrt{r^2 + R_s^2 + 2\sqrt{r^2 - (md)^2}\sqrt{R_s^2 - ((m-i)d)^2} + 2m(i-m)d^2} \\
&+ \mathbb{1}_{\{|i-m|d>R_s\}}(id), \\
\tilde{\gamma}_i =& \mathbb{1}_{\{|i-m|d<R_s\}} \sqrt{r^2 + R_s^2 - 2\sqrt{r^2 - (md)^2}\sqrt{R_s^2 - ((m-i)d)^2} + 2m(i-m)d^2} \\
&+ \mathbb{1}_{\{|i-m|d>R_s\}}(id), \\
& i = -\frac{N-1}{2}, \ldots, \frac{N-1}{2}.
\end{aligned}$$

*where $\mathbb{1}_{\{.\}}$ is the indicator function.*

*Proof.* Proof is similar to that of Theorem 2. □

As in the same lane transmitter case I can obtain approximations of the probability of success defined in the following corollaries.

**Corollary 3.** *The aggressive interference approximation of the probability of transmission success in a multi-lane highways with a transmitter located m lanes away*

*from the central lane is given by:*

$$\mathcal{P} \approx \frac{1}{\sqrt{R_t^2-(md)^2}} \int_{md}^{R_t} \frac{r}{\sqrt{r^2-(md)^2}} e^{-\frac{\mu T r^2 \kappa}{P}} \prod_{i=-\frac{N-1}{2}}^{\frac{N-1}{2}} \exp\left(-\sup_{\gamma}(c(\gamma,i))\Lambda \int_{\psi_i \in R^1} \left(\frac{1}{1+(\frac{\gamma_i}{rT^{1/\eta}})^{\eta}}\right) d\gamma_i\right) dr,$$

$$\stackrel{(\eta=2)}{=} \frac{1}{\sqrt{R_t^2-(md)^2}} \int_{0}^{R_t} \frac{r}{\sqrt{r^2-(md)^2}} e^{-\frac{\mu T r^2 \kappa}{P}} \prod_{i=-\frac{N-1}{2}}^{\frac{N-1}{2}} e^{-\tilde{\Lambda}(\hat{\gamma}_i,i)\sqrt{T}r \arctan\frac{\sqrt{T}r}{\hat{\gamma}_i} - \tilde{\Lambda}(\tilde{\gamma}_i,i)\sqrt{T}r \arctan\frac{\sqrt{T}r}{\tilde{\gamma}_i}} dr \tag{3.16}$$

*where $\psi_i$,$\hat{\gamma}_i$ and $\tilde{\gamma}_i$ are given in* Theorem 3.

Similarly, I can obtain the conservative interference approximation for the success probability as follows:

**Corollary 4.** *The conservative interference approximation of the probability of transmission success in a multi-lane highways with a transmitter located m lanes away from the central lane is given by:*

$$\mathcal{P} \approx \frac{1}{\sqrt{R_t^2-(md)^2}} \int_{md}^{R_t} \frac{r}{\sqrt{r^2-(md)^2}} e^{-\frac{\mu T r^2 \kappa}{P}} \prod_{i=-\frac{N-1}{2}}^{\frac{N-1}{2}} \exp\left(-\Lambda \int_{\psi_i \in R^1} \left(\frac{1}{1+(\frac{\gamma_i}{rT^{1/\eta}})^{\eta}}\right) d\gamma_i\right) dr,$$

$$\stackrel{(\eta=2)}{=} \frac{1}{\sqrt{R_t^2-(md)^2}} \int_{0}^{R_t} \frac{r}{\sqrt{r^2-(md)^2}} e^{-\frac{\mu T r^2 \kappa}{P}} \prod_{i=-\frac{N-1}{2}}^{\frac{N-1}{2}} e^{-\Lambda\sqrt{T}r \arctan\frac{\sqrt{T}r}{\tilde{\gamma}_i} - \Lambda\sqrt{T}r \arctan\frac{\sqrt{T}r}{\tilde{\gamma}_i}} dr \tag{3.17}$$

*where $\psi_i$,$\hat{\gamma}_i$ and $\tilde{\gamma}_i$ are given in* Theorem 3.

## 3.5 Numerical Results

In this section, I will first validate the analysis and then compare the proposed approach with the widely used approach in the literature. To this end, I will show that there exist an optimal value for the spectrum sensing threshold that maximizes the transmission capacity.

### 3.5.1 System Parameters and Model Validation

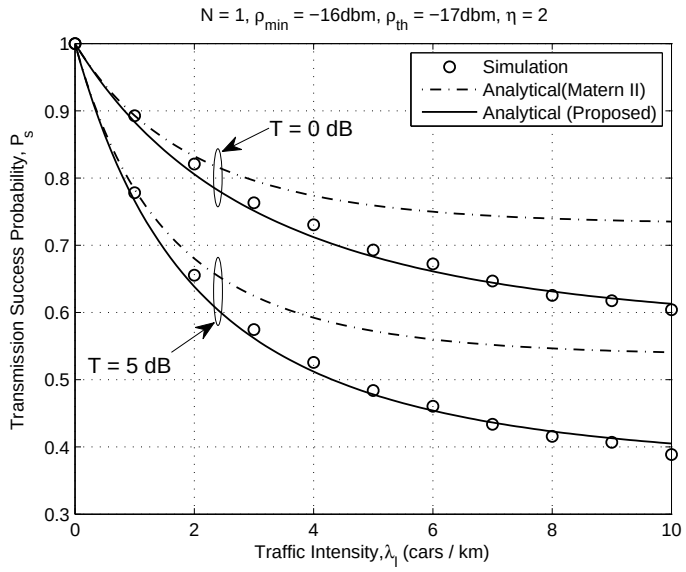


Figure 3.9: Model validation.

In the simulation model, I realize a network of vehicles on the lines according to a PPP. A transmitter is randomly selected whose average transmission range covers the test receiver at the origin. All vehicles use CSMA MAC protocol. The signal and interference powers are calculated at the origin and the SINR is evaluated. Unless otherwise stated, the simulation parameters are selected as; transmission power ($P = 1$ W), noise floor ($\kappa = -100dB$), road Length ($L = 10$ km), inter-lane distance ($d = 5$ m), sensing threshold ($\rho_{th} = -17$ dBm), receiver sensitivity ($\rho_{min} = -16$ dBm), path loss exponent ($\eta = 2$). The simulation is averaged over $10^4$ network realizations.

Fig.3.9 shows the success probability plotted against the traffic intensity $\lambda_l$ for $N = 1$. It effectively validates the proposed analysis methodology and also exposes the interference underestimation problem of the MHCPP-II even in the case of a single traffic lane. The results for the success probability in multi-lane highways ($N = 21$) are shown in Fig.3.10(a & b) for both sparse ($\lambda_l = 5$ cars/km) and dense traffic ($\lambda_l = 30$ cars/km) scenarios. It can be observed that for sparse traffic situations, the conservative interference approximation is a good estimate of the success probability. On the other hand, for dense traffic situations, the aggressive interference approximation tends to be a closer approximation. For intermediate traffic situations, the probability of success lies between the conservative and the aggressive interference approximation curves. Fig.3.10(a & b) also show that the SLA model using the MHCPP-II, which is widely used in literature, provides an optimistic measure of the success probability due to the underestimated interference. I exploit the developed framework to optimize the CSMA sensing threshold $\rho_{th}$. The transmission capacity metric [47], defined as the intensity of successful transmission per unit length, is used to balance the tradeoff imposed by $\rho_{th}$. For a fixed transmission range, the product of success probability and the intensity of concurrent transmitters is plotted for different inter-lane separations in Fig.3.11. The lane separation ranges from the standard $3.6m$ road width [48] in multi-lane highways to larger distances. The sensing threshold corresponding to the maximum value of each curve is the optimum sensing threshold. Fig.3.11 also exposes a critical value of $\rho_{th}$ i.e. $\rho_{critical}$ beyond which the analysis for different inter-lane distances coincide. In other words, if the sensing range is larger than the one corresponding to $\rho_{critical}$, I can safely use the SLA model without loss of accuracy. This is an important result since it specifies the condition for the validity of the widely used SLA model.

## 3.6 Conclusion

A novel analytical framework for modeling CSMA based inter-vehicle communication in multi-lane highways has been presented. The developed model is based on stochastic geometry and point process theory. An approximate yet accurate expressions for the intensity of concurrent transmitters and packet success probability have been obtained. The results show that the line abstraction model is not always an accurate assumption and that the widely accepted Matérn hard core point process underestimates the interference. Finally, I show the existence of an optimal spectrum sensing threshold for the CSMA protocol that balances the tradeoff between the success probability and spatial frequency reuse efficiency.

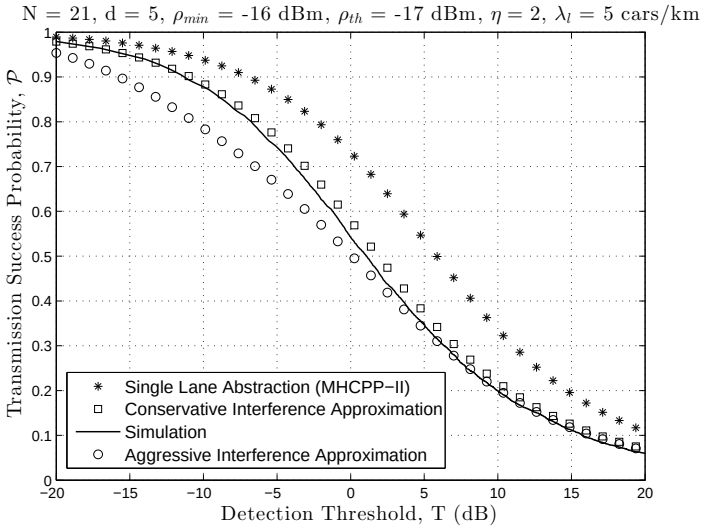


(a) Success Probability for multi-Lane Highway (N = 21) under sparse traffic.

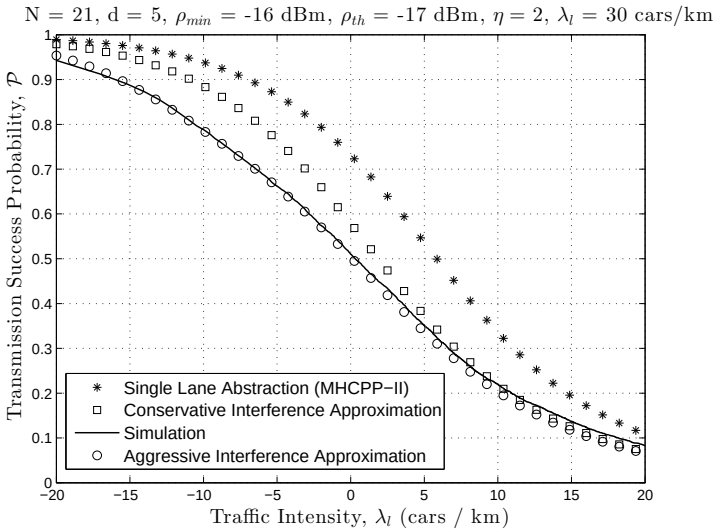


(b) Success Probability for multi-Lane Highway (N = 21) under dense traffic.

Figure 3.10: Success Probability against Traffic Intensity and Detection Threshold for Multi-Lane Highway.

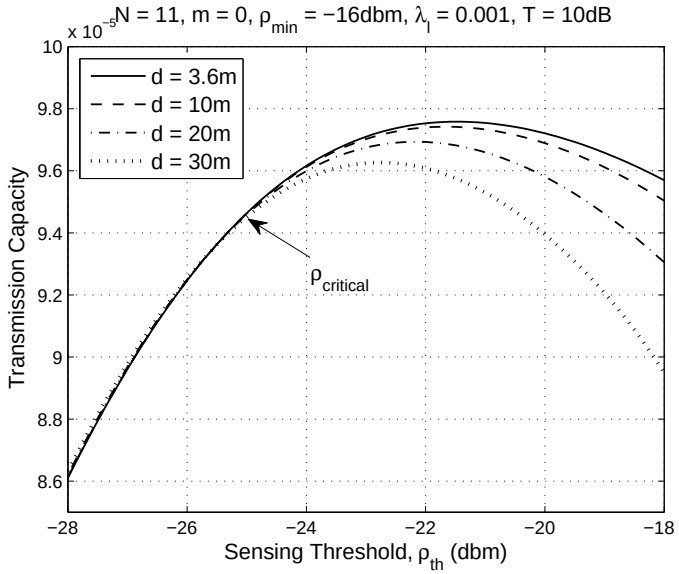


Figure 3.11: Optimizing sensing range of vehicles for different inter-lane distances

# Chapter 4

# Modeling and Analysis of Inter-vehicle Communication in Multi-Lane Highways with un-saturated transmission buffers

## 4.1 Introduction

In this chapter, the assumption of saturated transmission buffers used in chapter 3 i.e. each vehicle always has a packet to transmit, has been relaxed. Instead it is assumed that each node will transmit with a certain probability, known as the transmission probability or the probability of having a non-empty buffer. The transmission probability has been obtained using queueing theory analysis and has been incorporated into the developed framework in this thesis. The results in chapter 3 have been repeated under the unsaturated buffer case and insights have been drawn.

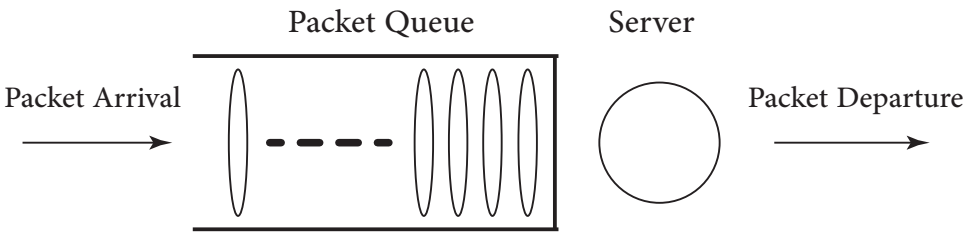


Figure 4.1: Single node queueing system.

## 4.2 System Model

Consider a single node queueing system as shown in Fig. 4.1 in which there is a single node or server that is processing the requests. In our case, each vehicle maintains a buffer of packets, of size $n$, that are ready to be transmitted and the channel acts as the server. As soon as the channel is idle, the packets are sent through the channel and if the packet is transmitted successfully at the receiver, the packet leaves the queue and the next packet in the buffer is processed. In case of unsuccessful transmission, the packet is retransmitted until it has been successfully transmitted.

To model this packet transmission, the Geo/Geo/1 discrete time Markov chain queueing system [49] is used. The packets arrival and departure is modeled by the discrete time birth death (BD) process. This means that at any single instant of time, there can be one birth i.e. packet entering the system, and one death i.e. packet leaving the system. The packet arrival probability, denoted by $p_A$ is the probability that a packet enters the buffer. This is assumed to be constant and depends on the application that is being used by the vehicular network. The probability of completion, denoted by $p_B$ is the probability that a packet is successfully processed and leaves the system. A packet is successfully processed if the channel is sensed as idle and the resulting transmission is successful. Therefore $p_B$ can be written as:

$$p_B = \mathcal{P}_{idle} \times \mathcal{P}, \tag{4.1}$$

where $\mathcal{P}_{idle}$ is the probability that the channel is in idle state and $\mathcal{P}$ is the transmission success probability as defined in chapter 4. In the following section, the probability that a vehicle has a non-empty buffer i.e. has a packet to send, denoted by $p$ is evaluated using queueing theory analysis.

## 4.3 Methodology

For brevity of notation, I denote $p_A$ as simply $a$, $p_B$ as $b$, $1-p_A$ as $\bar{a}$ and $1-p_B$ as $\bar{b}$. Let $x_i$ denote the probability that $i$ packets are waiting in the buffer to be processed. $p$ is the transmission probability. Using the algebraic approach used in [49], I can write the following probabilities as follows:

$$x_0 = x_0\bar{a} + x_1\bar{a}b \tag{4.2}$$

$$x_1 = x_0 a + x_1(\bar{a}\bar{b} + ab) + x_2\bar{a}b \tag{4.3}$$

$$x_i = x_{i-1}a\bar{b} + x_i(\bar{a}\bar{b} + ab) + x_{i+1}\bar{a}b, \qquad i > 2 \tag{4.4}$$

If I denote $\theta = \frac{a\bar{b}}{\bar{a}b}$, then

$$x_i = \frac{\theta^i}{\bar{b}} x_0, i \geq 1. \tag{4.5}$$

Using the normalization condition i.e. $\sum_{i=0}^{n} x_i = 1$,

$$\begin{aligned} x_0 + \sum_{i=1}^{n} \frac{\theta^i}{\bar{b}} x_0 &= 1, \\ x_0 &= \frac{1}{1 + \sum_{i=1}^{n} \frac{\theta^i}{\bar{b}}}, \\ x_0 &= \frac{a-b}{a(\frac{a\bar{b}}{b\bar{a}})^n - b}. \end{aligned} \tag{4.6}$$

Once the probability of an empty buffer is obtained, I can get the value of $p$ as

follows:

$$\begin{aligned} p &= 1 - x_0, \\ &= 1 - \frac{p_A - p_B}{p_A(\frac{p_A(1-p_B)}{p_B(1-p_A)})^n - p_B}. \end{aligned} \tag{4.7}$$

However, the value of $p$ depends on $p_B$, and $p_B$ depends on $\mathcal{P}_{idle}$ and $\mathcal{P}$ both of which also depend on $p$. Therefore the value of $p$ has to be obtained using an iterative algorithm as in [50]. The iterative procedure is described later in this section.

### 4.3.1 Intensity of Concurrent Transmitters

An unsaturated transmission buffer signifies that there will be time slots in which vehicles will not have packets to transmit despite the fact that the channel is idle. This means that the number of vehicles that transmit at the same time will be lesser than that calculated in chapter 3 in (3.4). Infact, the new intensity of transmitters incorporating the probability of non-empty buffer is as follows:

$$\begin{aligned} \Lambda &= p\lambda_l \frac{1 - e^{-p\mathbb{E}[|\mathcal{N}|]/2}}{p\mathbb{E}[|\mathcal{N}|]/2}, \\ &= p\lambda_l \mathcal{P}_{idle}. \end{aligned} \tag{4.8}$$

### 4.3.2 Iterative Algorithm

The probability of transmission (i.e. probability of having a non-empty buffer) can be evaluated using the iterative procedure in Algorithm 1.

## 4.4 Numerical Results

Using the queueing theory model for unsaturated transmission buffers, the developed framework in chapter 3 is modified and the results are repeated. The system model

**Algorithm 1** Algorithm to find transmission probability

**procedure**
Initialize by $p = 0.5$ and $p_A$ =constant.
*while: Not converged*
Calculate $\Lambda$ in (4.8).
Evaluate $\mathcal{P}$ based on the value of $\Lambda$.
Use $\mathcal{P}$ to calculate $p_B$ from (4.1).
Calculate $p$ using (4.7).

and simulation settings have been kept the same. I assume that the packet arrival probability for each vehicle, $p_A = 0.01$. Since the packet transmission time, including back-off delays, is in the order of milliseconds, this implies that the packets arrive at a rate of around 100 packets/second. The simulation parameters are selected as; transmission power ($P = 20$ dBm), noise floor ($\kappa = -104dBm$), road Length ($L = 10$ km), inter-lane distance ($d = 5$ m), sensing threshold ($\rho_{th} = -86$ dBm), receiver sensitivity ($\rho_{th} = -86$ dBm), path loss exponent ($\eta = 4$), packet queue size ($n = 100$). The simulation is averaged over $10^4$ network realizations.

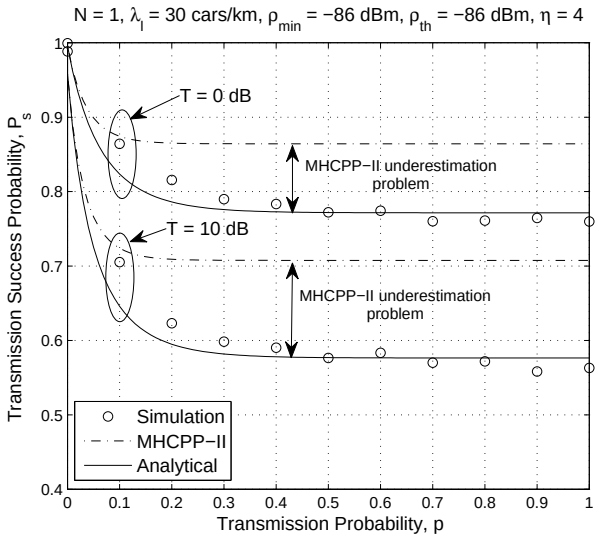


Figure 4.2: Model validation with unsaturated buffers.

Fig. 4.2 validates the developed framework with unsaturated buffers. Fig. 4.3 and Fig. 4.4 show that the proposed conservative interference approximation is tight under sparse traffic conditions and the aggressive interference approximation is a

good estimate under dense traffic conditions. Finally Fig. 4.5 shows that there exists a sensing threshold that maximizes the transmission capacity thus balancing off the tradeoff between probability of transmission success and the spatial frequency reuse efficiency.

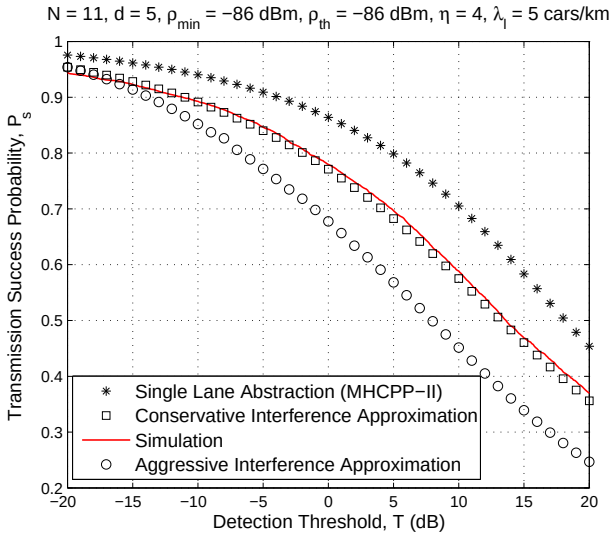


Figure 4.3: Success probability for multi-Lane highway (N=11) in sparse traffic with unsaturated buffers.

## 4.5 Conclusion

The results in this chapter clearly lead to the same conclusions as in chapter 3. It is observed that the incorporation of queueing analysis for the transmission probability unnecessarily complicates the analysis. Although the model with unsaturated transmission buffers is more realistic and provides plausible values for the probability of success, however it does not contribute much in the study of system tradeoffs. Therefore, I will ignore the unsaturated buffers and continue with the saturated buffers assumption in chapter 5 for modeling multi-hop communication.

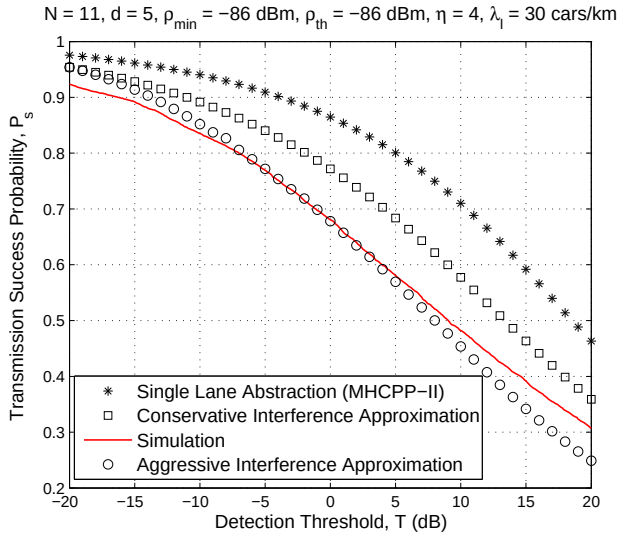


Figure 4.4: Success probability for multi-Lane highway (N=11) in dense traffic with unsaturated buffers.

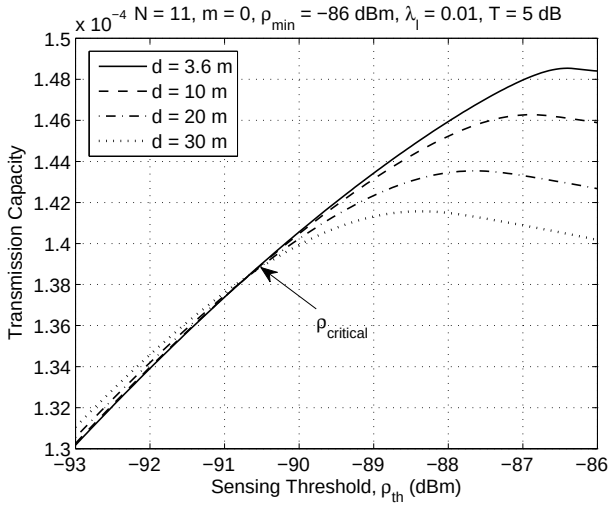


Figure 4.5: Optimizing sensing range of vehicles for different inter-lane distances (unsaturated buffers).

# Chapter 5

# Modeling & Analysis of Multi-hop communication in highway VANETs

## 5.1 Introduction

In this chapter, I model multi-hop vehicular communication in highways. The objective is to efficiently disseminate packets across the network by successively forwarding the packets to vehicles in a particular direction as illustrated in Fig. 5.1. There are several packet forwarding strategies that are studied in this chapter and the trade-offs imposed by selecting those strategies are discussed. The analysis developed in chapter 3 has been utilized to model the multi-hop IVC. Finally insights have been developed to identify the best forwarding strategy and tuning the sensing threshold to maximize the efficiency of packet dissemination.

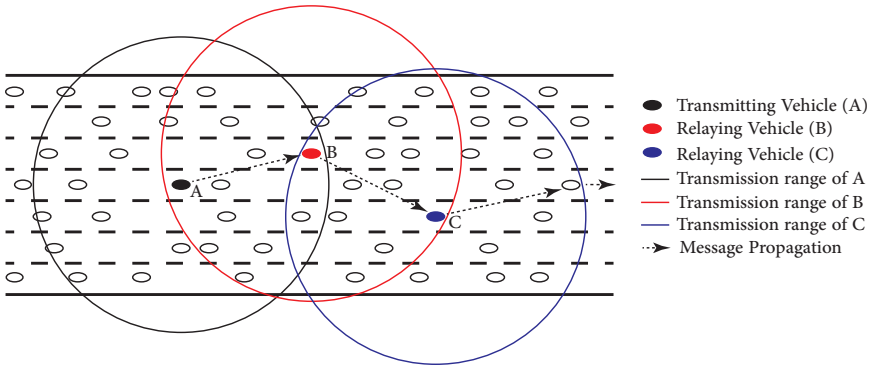


Figure 5.1: Message propagation using inter-vehicle communication

## 5.2 System Model

### 5.2.1 Network Model

The network model for the multi-hop scenario is similar to the one used in chapter 3. However it is worth describing it again in this chapter. I consider a multi-lane highway network constituted from $N$ parallel lanes separated by a fixed distance $d$. It is assumed that each traffic lane has an infinite length and is populated by vehicles according to an independent and homogeneous 1-D Poisson Point Process (PPP) of intensity $\lambda_l$, i.e. $\Phi_i = \{v_{ij}; j = 0, 1, 2, \ldots\}$, where $i = 1, \ldots, N$ is the lane index and $v_{ij}$ represents the location of the $j^{th}$ vehicle on the $i^{th}$ traffic lane. A snapshot of the network model is shown in Fig. 5.2.

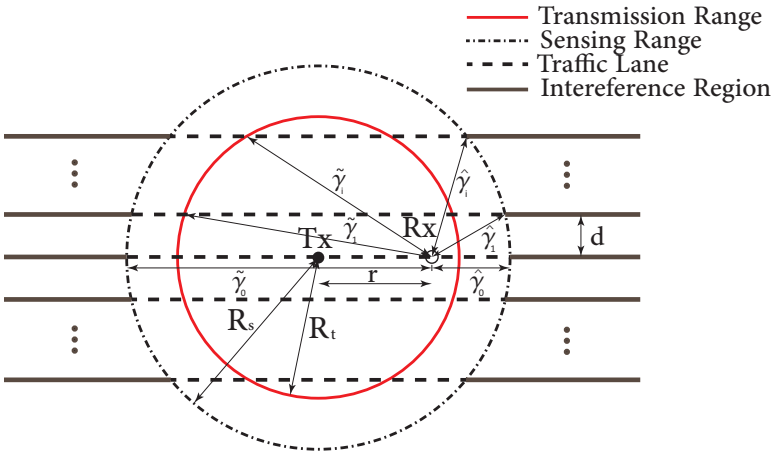


Figure 5.2: Multi-lane highway with test transmitter and receiver.

Each vehicle transmits with a fixed power $P$, or equivalently has a fixed transmission range $R_t$. The signal power decays with the distance according to the power law propagation model with a path-loss exponent $\eta > 1$. The transmission range can therefore be expressed as $R_t = (\frac{P}{\rho_{min}})^{1/\eta}$ where $\rho_{min}$ is the receiver sensitivity. Besides path loss attenuation, the signal power experiences fading which is assumed to be exponential with mean of $1/\mu$. I consider a signal capture model, which assumes that a packet can be correctly decoded by the receiver iff the signal-to-interference-plus-noise-ratio (SINR) exceeds a target threshold $T$.

The sensing threshold $\rho_{th}$ of the CSMA protocol is a system wide design parameter used by all vehicles. From a geometric perspective, $\rho_{th}$ can be directly translated to a sensing range, also denoted as the contention domain, represented by $R_s = (\frac{P}{\rho_{th}})^{1/\eta}$. The sensing range affects the spatial frequency reuse because the CSMA protocol does not allow the same channel to be used by two vehicles in the same contention domain, where the contention domain of a the $j^{th}$ vehicle on the $i^{th}$ lane ($v_{ij}$) is defined as $\mathcal{N}_{v_{ij}} = \{v_{mn} : P\|v_{ij} - v_{mn}\|^{-\eta} \geq \rho_{th}, \forall m, n\}$, where $\|.\|$ is the Euclidean norm. If $v_{ij}$ is in the contention domain of $v_{mn}$, then from the reciprocity of wireless networks, the converse is also true. Thus, for notational brevity, I will drop the subscripts of $v_{ij}$, and hereafter refer to the contention domain of a typical vehicle as $\mathcal{N}$. The average number of vehicles in the contention domain of a center-lane transmitter is given by:

$$\mathbb{E}\left[|\mathcal{N}|\right] = 2\lambda_l \left( R_s + 2 \sum_{i=1}^{(N-1)/2} \sqrt{R_s^2 - (id)^2} \right). \tag{5.1}$$

where $|.|$ represents the set cardinality. In a similar manner, I can define the transmission neighbourhood[1] of a typical node as $\mathbf{N}_{v_{ij}} = \{v_{mn} : P\|v_{ij} - v_{mn}\|^{-\eta} \geq \rho_{min}, \forall m, n\}$. The average number of neighbours of a test transmitter placed at the origin with

[1] vehicles inside the transmission range of each other are considered to be neighbours.

transmission range $R_t$ is, therefore

$$\mathbb{E}\left[|\mathbf{N}|\right] = 2\lambda_l \left( R_t + 2 \sum_{i=1}^{(N-1)/2} \sqrt{R_t^2 - (id)^2} \right). \tag{5.2}$$

## 5.3 Packet Forwarding Strategies

From a transmitter's perspective, there are several strategies to select the relaying vehicle from its neighbors. The most simple strategies are to transmit to either the nearest node, the farthest node, or to a random node inside the transmission range. I assume that the packets destination is located far enough such that the progress can be defined as the horizontal distance moved along the highway towards the receiver. I will only allow forward progress in which the message direction can be estimated with the aid of GPS (e.g., the location of the nearest emergency center in case of accidents). The different transmission strategies are described as follows:

### 5.3.1 Most Forward with Fixed Radius (MFR)

In this strategy, a typical transmitting node will forward the packet to the neighbour that results in the most forward progress within its transmission range. *MFR* maximizes the forward progress on the expense of low success probability due to the imposed large transmitter-receiver spacing. Note that *MFR* requires a conservative sensing threshold (i.e., $\zeta < R_s/R_t \geq 1$) such that the sensing range can provide sufficient interference protection for the receiver. Note also that a conservative sensing threshold implies low spatial frequency reuse.

### 5.3.2 Nearest with Forward Progress (NFP)

In this strategy, a typical transmitting node will forward the packet to its closest neighbour. This would increase the per-hop transmission success probability on the

expense of minimizing the forward progress. However, the *NFP* strategy can sustain an aggressive sensing threshold (i.e., $\zeta = R_s/R_t \ll 1$) due to the small link distance (i.e., short transmitter-receiver separation) which improves the desired signal received power.

### 5.3.3 Random with Forward Progress (RFP)

In this strategy, every potential receiver, that results in forward packet progress, has an equal probability of being selected by the protocol. This strategy achieves a midpoint performance between the *MFR* and the *NFP*.

## 5.4 Methodology of Analysis

### 5.4.1 SINR Characterization

Due to the shared nature of the wireless medium, SINR is a major performance metric. The per-hop transmission is considered successful (i.e., correctly decoded by the receiver) if the SINR is above a predefined threshold. The SINR can be written as:

$$\mathrm{SINR}_{\chi} = \frac{P h_o r_{\chi}^{-\eta}}{\kappa + \underbrace{\sum_{i=1}^{N} \sum_{v_{ij} \in \tilde{\Phi}_i \setminus v_0} P h_{ij} \left\| v_{ij} \right\|^{-\eta}}_{I_{agg}}}, \tag{5.3}$$

where $\chi \in \{M, N, R\}$ is the message forwarding mode, where $M$, $N$, and $R$ denote the *MFR*, the *NFP*, and *RFP* respectively. The distance $r_{\chi}$ denotes the transmitter-receiver separation when using $\chi$ forwarding scheme, the set $\tilde{\Phi}_i \setminus v_0 \subseteq \Phi_i$ denotes the set of active transmitters, excluding the intended transmitter $v_o$, which is obtained after dependent thinning of the original PPP due to the CSMA contention. $v_{ij} \in \mathbb{R}^2$ is the location of the $j^{th}$ interfering vehicle on the $i^{th}$ traffic lane. Finally, $h_o$ and $h_{ij}$

are i.i.d. random variables representing the channel fading between the test transmitting vehicle and the selected receiver and between the receiver and $ij^{th}$ interfering vehicle respectively, and $\kappa$ is the noise variance. From (5.3), it can directly observed that SINR is a random variable that includes several uncertainties which are, the vehicles' locations, the channel gains, the CSMA contention based access, as well as the transmitter-receiver separation. The complementary cumulative distribution function (*ccdf*) of the SINR defines the per-hop transmission success probability, which can be calculated as follows:

$$\begin{aligned}\mathcal{P}_\chi &= \mathbb{P}\left\{SINR_\chi > T\right\} \\ &= \int_r \exp\left\{-\frac{T\mu\kappa r^\eta}{P}\right\} \mathcal{L}_{I_{agg}}\left(\frac{T\mu r^\eta}{P}\right) f_{r_\chi}(r)dr, \end{aligned} \tag{5.4}$$

where $\mathcal{L}_{I_{agg}}(.)$ is the Laplace transform[2] (LT) of $I_{agg}$. Equation (5.4) shows the auxiliary metrics that are required to evaluate the per-hop success probability, namely, the transmitter-receiver separation distance distribution $f_{r_\chi}(.)$ and the LT of the aggregate interference $I_{agg}$. Note the the LT of the aggregate interference is a function of the intensity of concurrent transmitters (or interferers).

### 5.4.2 Distance Distribution

Since the receiver selection is based on the underlying message forwarding protocol, the transmitter-receiver separation distance distribution is different for *MFR*, *NFP*, and *RFP*. For the *MFR* the transmitter-receiver separation distance distribution is estimated via the following lemma:

**Lemma 7.** *The distribution of the distance $r_M$ between the transmitter and the re-*

[2]with a slight abuse of the terminology, I will denote the LT of the *pdf* of $I_{agg}$ as the LT of $I_{agg}$.

*ceiver in the* MFR *strategy is distributed as follows:*

$$f_{r_M}(r) = \begin{cases} \frac{\lambda_l e^{-\lambda_l \mathbf{A}(r)}}{1-e^{\mathbb{E}[|\mathbf{N}|/2]}} & 0 < r \leq d \\ \frac{\lambda_l e^{-\lambda_l \mathbf{A}(r)}}{1-e^{\mathbb{E}[|\mathbf{N}|/2]}} + \frac{2\lambda_l r \exp\left(-\lambda_l \mathbf{A}\left(\sqrt{r^2-d^2}\right)\right)}{(1-e^{\mathbb{E}[|\mathbf{N}|/2]})\sqrt{r^2-d^2}} & d < r \leq 2d \\ \vdots & \\ \frac{\lambda_l e^{-\lambda_l \mathbf{A}(r)}}{1-e^{\mathbb{E}[|\mathbf{N}|/2]}} + & \\ \sum\limits_{i=1}^{(N-1)/2} \frac{2\lambda_l r \exp\left(-\lambda_l \mathbf{A}\left(\sqrt{r^2-(id)^2}\right)\right)}{(1-e^{\mathbb{E}[|\mathbf{N}|/2]})\sqrt{r^2-(id)^2}}. & \frac{(N-1)d}{2} < r \leq R_t \end{cases} \tag{5.5}$$

*Proof.* See **Appendix E** □

For the *NFP* strategy, the distribution of the transmitter-receiver distance is stated via the following lemma:

**Lemma 8.** *The distribution of the distance $r_N$ between the transmitter and the receiver for the* NFP *strategy is distributed as:*

$$f_{r_N}(r) = \begin{cases} \frac{\lambda_l e^{-\lambda_l \mathbf{B}(r)}}{1-e^{\mathbb{E}[|\mathbf{N}|/2]}} & 0 \leq r \leq d \\ \frac{\lambda_l e^{-\lambda_l \mathbf{B}(r)}}{1-e^{\mathbb{E}[|\mathbf{N}|/2]}} 0 \leq r \leq d + \frac{2\lambda_l r \exp\left(-\lambda_l \mathbf{B}\left(\sqrt{r^2-d^2}\right)\right)}{\sqrt{r^2-d^2}} & d < r \leq 2d \\ \vdots & \\ \frac{\lambda_l e^{-\lambda_l \mathbf{B}(r)}}{+} & \\ \sum\limits_{i=1}^{(N-1)/2} \frac{2\lambda_l r \exp\left(-\lambda_l \mathbf{B}\left(\sqrt{r^2-(id)^2}\right)\right)}{(1-e^{\mathbb{E}[|\mathbf{N}|/2]})\sqrt{r^2-(id)^2}}. & \frac{(N-1)d}{2} < r \leq R_t \end{cases} \tag{5.6}$$

*Proof.* See **Appendix F** □

The transmitter-receiver separation distance distribution for the *RFP* is calculated via the following lemma:

**Lemma 9.** *The distribution of the distance $r_M$ between the transmitter and the re-*

*ceiver for the* RFP *strategy is distributed as:*

$$f_{r_R}(r) = \begin{cases} \frac{1}{NR_t}, & 0 \leq r \leq d, \\ \frac{1}{NR_t} + \frac{2r}{NR_t\sqrt{r^2-d^2}}, & d < r \leq 2d, \\ \vdots & \\ \frac{1}{NR_t} + \sum_{i=1}^{(N-1)/2} \frac{2r}{NR_t\sqrt{r^2-(id)^2}}, & 2d < r \leq R_t. \end{cases} \tag{5.7}$$

*Proof.* See **Appendix G** □

## 5.5 Performance Analysis

In this section I will evaluate the system performance for each of the transmission strategies based on the following metrics:

1. Probability of Transmission Success ($\mathcal{P}$)
2. Normalized Average Forward Progress (NAFP)
3. Aggregate Packet Progress (APP)

In the following subsections, I define these metrics along with the analysis for the different transmission strategies.

### 5.5.1 Probability of Transmission Success

The probability of transmission success is defined as the probability that the *SINR* at the receiver is above a particular threshold. The general framework for evaluating the probability of transmission success has been explained in Section 5.4.1. For $N-$lane highway with an inter-lane separation $d$, the probability of transmission success is

given as follows:

$$\mathcal{P}_{\chi} = \int_{0}^{R_t} e^{-\frac{\mu T r^{\eta} \kappa}{P}} \prod_{i=-\frac{N-1}{2}}^{\frac{N-1}{2}} \exp\left( - \int_{\psi_i \in R^1} \left( \frac{\tilde{\Lambda}(\gamma_i, i)}{1 + (\frac{\gamma_i}{r T^{1/\eta}})^{\eta}} \right) d\gamma_i \right) f_{r_{\chi}}(r) dr, \tag{5.8}$$

for $\chi = \{M, N, R\}$. $\mathbb{1}_{\{.\}}$ is the indicator function that is equal to 1, if the condition in the braces is true, and 0 otherwise.

However, as in chapter 3, the exact analytical evaluation of the expression in (5.8) for the multi-lane case is not possible. This has been discussed in chapter 3 and two approximations have been proposed to overcome this analytical difficulty. For the special case where $\eta = 2$, I can obtain the aggressive interference approximation and the conservative interference approximation using the following corollaries:

**Corollary 5.** *The aggressive interference approximation for the probability of transmission success in an $N-$lane highway according to the packet forwarding strategy selected is given by:*

$$\mathcal{P}_{\chi} \approx \int_{0}^{R_t} e^{-\frac{\mu T r^2 \kappa}{P}} \prod_{i=0}^{(N-1)/2} e^{-(1+\mathbb{1}_{\{i>0\}}) \tilde{\Lambda}(\hat{\gamma}_i, i) \sqrt{T} r \tan^{-1} \frac{\sqrt{\mathrm{T}}\mathrm{r}}{\hat{\gamma}_\mathrm{i}}} e^{-(1+\mathbb{1}_{\{i>0\}}) \tilde{\Lambda}(\tilde{\gamma}_i, i) \sqrt{T} r \tan^{-1} \frac{\sqrt{\mathrm{T}}\mathrm{r}}{\tilde{\gamma}_\mathrm{i}}} f_{r_{\chi}}(r) dr, \tag{5.9}$$

*for $\chi = \{M, N, R\}$. The parameters $\hat{\gamma}_i$ and $\tilde{\gamma}_i$ are illustrated in Fig. 5.2 and their values can be expressed as follows:*

$$\begin{aligned} \hat{\gamma}_i &= \sqrt{r^2 + R_s^2 + 2R_s\sqrt{r^2 - (id)^2}}, \\ \tilde{\gamma}_i &= \sqrt{r^2 + R_s^2 - 2R_s\sqrt{r^2 - (id)^2}}, \qquad i = 0, 1, \ldots, \frac{N-1}{2}. \end{aligned} \tag{5.10}$$

**Corollary 6.** *The conservative interference approximation for the probability of transmission success in an $N-$lane highway according to the packet forwarding strategy*

*selected is given by:*

$$P_\chi \approx \int_0^{R_t} e^{-\frac{\mu T r^2 \kappa}{P}} e^{-N\Lambda\sqrt{T}r\tan^{-1}\frac{\sqrt{\mathrm{T_r}}}{\mathrm{R_s}-\mathrm{r}}} e^{-N\Lambda\sqrt{T}r\tan^{-1}\frac{\sqrt{\mathrm{T_r}}}{\mathrm{R_s}+\mathrm{r}}} f_{r_\chi}(r)dr, \tag{5.11}$$

*for* $\chi = \{M, N, R\}$.

### 5.5.2 Normalized Average Forward Progress

The forward progress is defined as the average distance traveled by the packet towards its final destination. Note that I assume the destination is located infinitely far away and therefore the horizontal distance covered can be reasonably used as a measure of progress towards the destination. The packet progress is an important measure because it signifies the number of transmissions required for transmitting a packet from source to destination over a multi-hop network and hence the transmission time. I are interested in successful packet progress because the progress will only be made if the transmission is successful. Hence the probability of transmission success is implicit when I use the forward progress metric. The average forward progress denoted by $\bar{\mathrm{Z}}_\chi$, is defined as follows:

$$\bar{\mathrm{Z}}_\chi = \mathcal{P}_\chi \times \mathbb{E}[\mathrm{Z}_\chi] \tag{5.12}$$

where $\mathbb{E}[\mathrm{Z}_\chi]$ is the expected forward progress in case of a successful transmission. The expected forward progress per hop for the *MFR*, *NFP* and the *RFP* are given by (5.13), (5.14) and (5.15) respectively.

Similar to [51], to make the average forward progress dimensionless, I normalize it by the average distance between two nearest neighbours. In this way, I transform the notion of distance (in meters) to the notion of hops (or number of nodes crossed over under a single transmission). The distance between two nearest nodes is given

$$\mathbb{E}[\mathrm{Z}_M] = \frac{N}{e^{\frac{\mathbb{E}[\mathbf{N}]}{2}} - 1} \left[ \sum_{i=0}^{\frac{N-1}{2}} \left( \frac{\exp\left(2\lambda_l \sum_{j=0}^{i} \omega(j)\right) \left(1 - \lambda_l (N-2i)\omega(i)\right) e^{\lambda_l (N-2i)\omega(i)}}{\lambda_l (N-2i)^2} + \frac{\exp\left(2\lambda_l \sum_{j=0}^{i} \omega(j)\right) \left(\lambda_l (N-2i)\omega(i+1) - 1 e^{\lambda_l (N-2i)\omega(i+1)}\right)}{\lambda_l (N-2i)^2} \right) \right] \tag{5.13}$$

$$\mathbb{E}[\mathrm{Z}_N] = \frac{N}{1 - e^{-\frac{\mathbb{E}[|\mathbf{N}|]}{2}}} \left[ \sum_{i=0}^{\frac{N-1}{2}} \left( \frac{\exp\left(-2\lambda_l \sum_{j=0}^{i} \omega(j)\right) \left(1 + \lambda_l (N-2i)\omega(i)\right) e^{-\lambda_l (N-2i)\omega(i)}}{\lambda_l (N-2i)^2} - \frac{\exp\left(-2\lambda_l \sum_{j=0}^{i} \omega(j)\right) \left(1 + \lambda_l (N-2i)\omega(i+1)\right) e^{-\lambda_l (N-2i)\omega(i+1)}}{\lambda_l (N-2i)^2} \right) \right] \tag{5.14}$$

$$\mathbb{E}[\mathrm{Z}_R] = \frac{1}{2} \sum_{i=1}^{\frac{N-1}{2}} \left( \frac{1}{N R_t} + \Omega(i) \right) \left( \omega(i+1)^2 - \omega(i)^2 \right) \tag{5.15}$$

Note:

$$\omega(i) = \begin{cases} 0, & i = 0 \\ \sqrt{R_t^2 - \left(\frac{N-(2i-1)}{2} d\right)^2}, & otherwise. \end{cases} \tag{5.16}$$

$$\tag{5.17}$$

$$\Omega(i) = \begin{cases} 0, & i = \frac{N-1}{2} \\ \sum_{i=1}^{\frac{N-(2i-1)}{2}} \frac{2}{N\sqrt{R_t^2 - (id)^2}}, & otherwise. \end{cases} \tag{5.18}$$

*Proof.* See **Appendix H** □

by (F.7). Thus I can conveniently use $\bar{\mathrm{Z}}_\chi \lambda_l$ as a measure of the normalized average forward progress made in a single transmission in terms of the number of nodes crossed over.

### 5.5.3 Aggregate Packet Progress

The aggregate packet progress (APP) metric is defined as the product of the number of successful local transmissions per unit distance, denoted by $C$, and the expected forward progress, measured in distance per every local transmission. Note that APP is dimensionless and can be expressed mathematically as:

$$APP_\chi = C \times \mathbb{E}[\mathrm{Z}_\chi] = \bar{\mathrm{Z}}_\chi \Lambda \tag{5.19}$$

The number of successful local transmissions per unit distance, also known as the transmission capacity is defined by the product of the probability of transmission success and the intensity of concurrent transmitters:

$$C(\rho_{th}) = \mathcal{P}_\chi(\rho_{th}) \times \Lambda(\rho_{th}) \tag{5.20}$$

The transmission capacity $C$, is a function of the sensing threshold $\rho_{th}$. The probability of success is an increasing function of the sensing range because of the receding interferers, hence an decreasing function of $\rho_{th}$. On the other hand, the intensity of concurrent transmitters is a decreasing function of the sensing range and thus an increasing function of $\rho_{th}$. To this end, I will show that there exists an optimal value of $\rho_{th}$ that maximizes the APP performance metric under the different forwarding strategies.

## 5.6 Simplifying Approximations

While the PPP approximation in *Assumption 3* is mandatory for the proposed analysis, there are some approximations which can be used to simplify and to gain insight into the more elaborate expressions used in this thesis. I begin with the expressions of the distance distribution between the transmitter and receiver. The distance distribution for the *MFR* forwarding protocol given by (5.5) can be approximated as:

$$f_{r_M}(r) \approx \begin{cases} 0, & 0 < r \leq \frac{(N-1)d}{2}, \\ \frac{\lambda_l e^{-\lambda_l \mathbf{A}(r)}}{1-e^{\mathbb{E}[|\mathbf{N}|/2]}} + & \\ \sum\limits_{i=1}^{(N-1)/2} \frac{2\lambda_l r e^{-\lambda_l \mathbf{A}\left(\sqrt{r^2-(id)^2}\right)}}{(1-e^{\mathbb{E}[|\mathbf{N}|/2]})\sqrt{r^2-(id)^2}}, & \frac{(N-1)d}{2} < r \leq R_t. \end{cases} \tag{5.21}$$

This approximation is based on the fact that the receiver, in the case of the *MFR* forwarding strategy, will be located near the edge of the transmission range with high probability and thus one part of the pdf dominates resulting in this approximation which is tight for higher intensities. Similarly for the *NFP* forwarding strategy, I can approximate the distance distribution given by (5.6) as follows:

$$f_{r_N}(r) \approx \frac{N\lambda_l e^{-\lambda_l \mathbf{B}(r)}}{1-e^{\mathbb{E}[|\mathbf{N}|/2]}}, \qquad 0 < r \leq R_t. \tag{5.22}$$

This approximation is based on the nature of the *NFP* strategy which dictates a receiver located very close to the transmitter, thus there is a higher probability of small transmitter receiver distances which leads to the above approximation.

The expressions for the expected forward progress given in (5.13),(5.14) and (5.15) , are also involved and can be simplified to gain insight. The expected forward progress for the *MFR* forwarding can be approximated as:

$$\mathbb{E}\left[\mathrm{Z}_M\right] \approx \frac{1+\exp(N\lambda_l R_t)(N\lambda_l R_t - 1)}{N\lambda_l(\exp(\mathbb{E}[\mathbf{N}]/2))} \tag{5.23}$$

This follows from using the approximation for $\mathbf{A}(\mathrm{z})$ given by (E.4) under the assump-

tion that $R_t >> \frac{(N-1)d}{2}$[3]. Similarly, using the approximation for $\mathbf{B}(z)$ given by (F.3) leads to the approximate average forward progress for the *NFP* forwarding strategy as:

$$\mathbb{E}\left[\mathrm{Z}_N\right] \approx \frac{1-\exp(-N\lambda_l R_t)(N\lambda_l R_t+1)}{N\lambda_l} \tag{5.24}$$

Finally, using the same assumption, the expected forward progress for the *RFP* strategy can be obtained using (G.3) as:

$$\mathbb{E}\left[\mathrm{Z}_R\right] \approx \frac{R_t}{2}. \tag{5.25}$$

## 5.7 Numerical Results & Discussion

In this section, I will first validate the proposed analysis and then provide numerical results to compare the performance of the three forwarding strategies on the metrics defined in Section 5.5. I will also show that there is an optimum sensing threshold that maximizes the transmission capacity as well as the forward progress.

### 5.7.1 System Parameters and Model Validation

Throughout this section, I use the number of traffic lanes in the multi-lane highway $N = 11$ with an inter-lane distance $d = 5m$ to investigate wide highways. The transmission range used is $R_t = 200m$ and is suitable for typical applications of inter-vehicular communication. The path loss exponent used in the analysis and simulation is $\eta = 2$. For the purpose of simulation, I assume a $10km$ length of parallel road segment. The vehicles are distributed on the roads as linear Poisson Point Processes. The intensity of vehicles used in this thesis ranges from 0 to 30 vehicles per $km$. More

[3]This is a reasonable assumption since a vehicle on one edge of the highway should be able to communicate to the roadside base stations located near the opposite edge of the highway

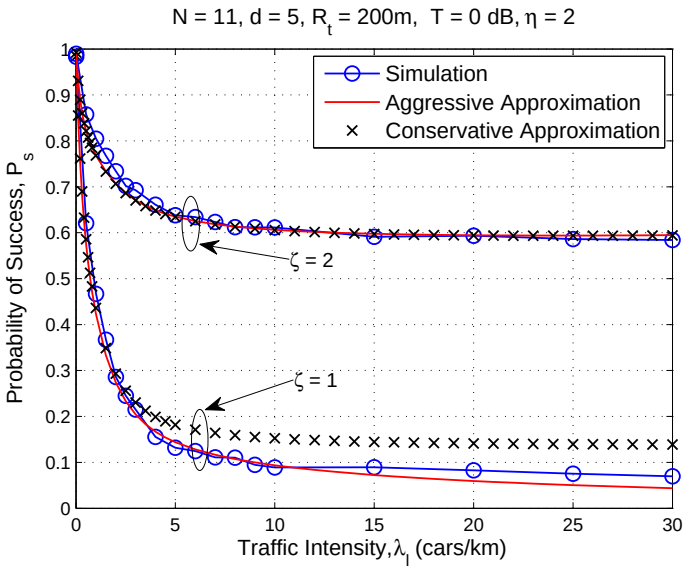


Figure 5.3: Model validation for the *MFR* strategy

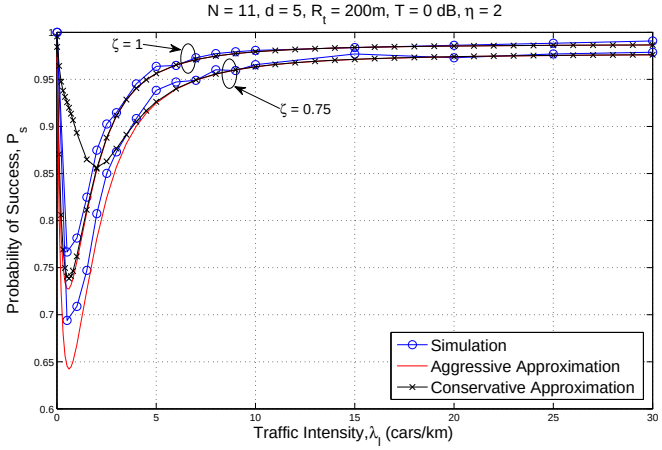


Figure 5.4: Model validation for the *NFP* strategy

simulation parameters used in the results are listed in Table 5.1.

In the simulation model, I realize a network of vehicles on a set of parallel lines according to a PPP. A test transmitting vehicle placed at the origin selects one of its neighbours as a receiver, based on the transmission strategy selected. Since the transmitters are using CSMA MAC protocol, no vehicle can transmit if another vehicle in its neighborhood is already transmitting. I assume that all vehicles have packets to transmit at all times. The signal and interference powers are calculated at the receiver and the SINR is evaluated. The simulation is averaged over $10^4$ realizations.

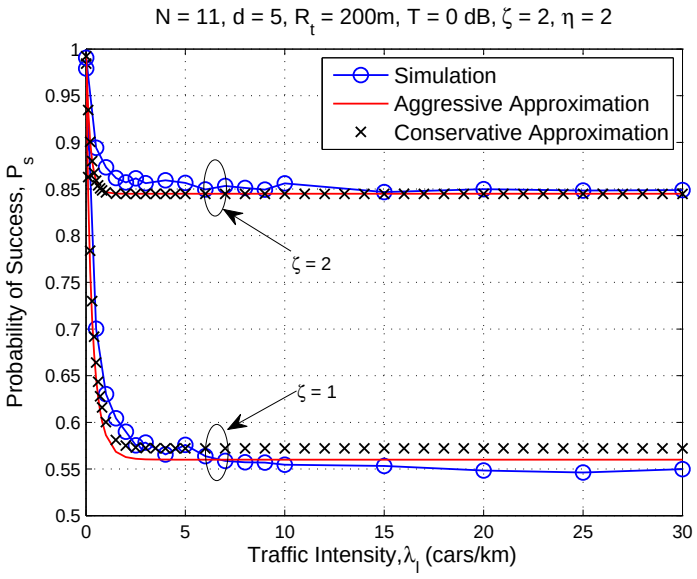


Figure 5.5: Model validation for the *RFP* strategy

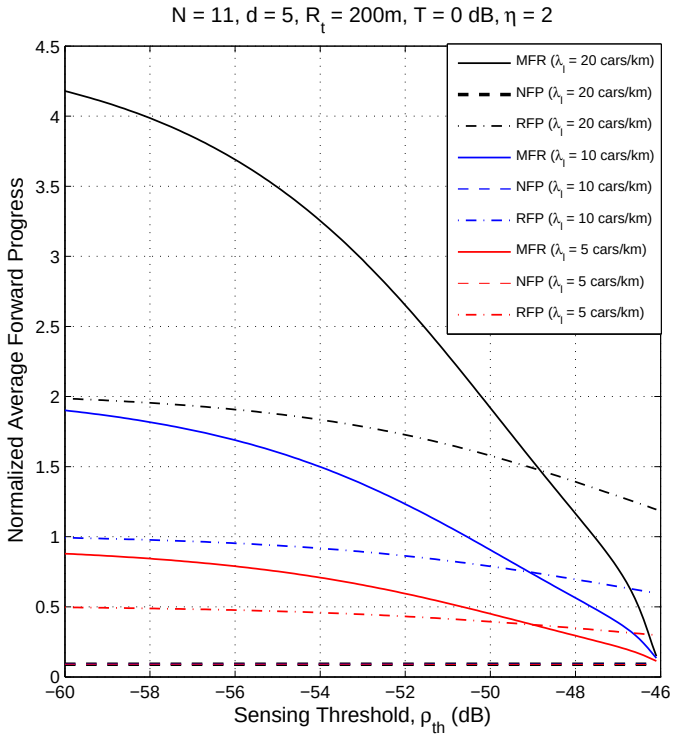


Figure 5.6: Normalized average forward progress against sensing range

Fig. 3.2 shows the simulation results of the success probability for the *MFR* strategy using three modeling approaches mentioned in Section 3.2.1. It is clear that, for large number of traffic lanes, the SLA model is not an accurate model. However

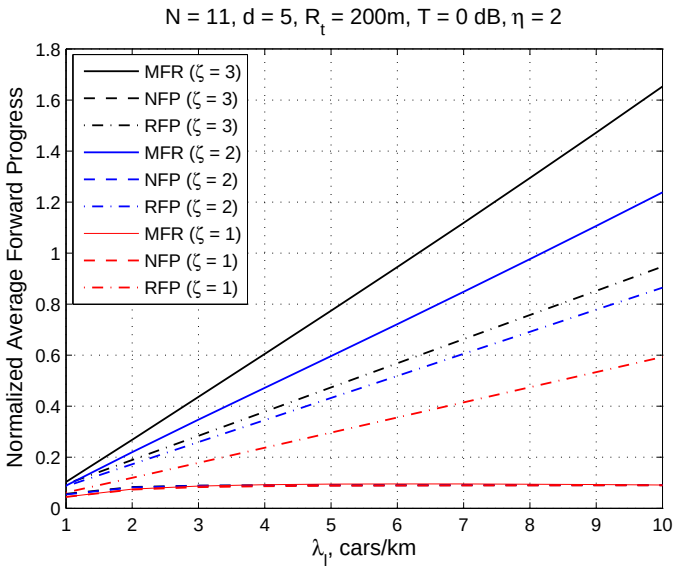


Figure 5.7: Normalized average forward progress for different traffic intensities

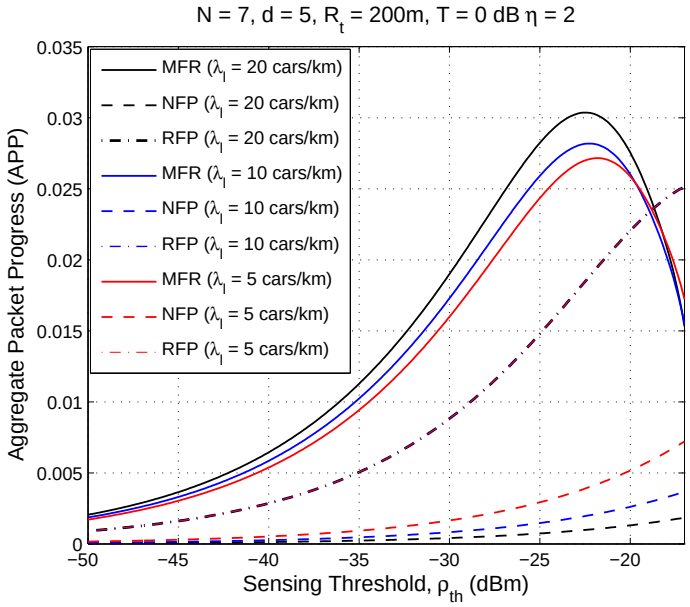


Figure 5.8: Maximizing transmission capacity and forward progress

the multi-lane model and the 2D-PPP model are almost equivalent in terms of the probability of success. The results in Fig. 5.3, 5.4 and 5.5 effectively validate the proposed analysis. It can be observed in general for all strategies that the aggressive approximation is a good approximation for small values of $\zeta$. However for higher values of $\zeta$, the conservative approximation and the aggressive approximation become

Table 5.1: Simulation Parameters

| Parameter | Value |
|---|---|
| Carrier frequency | $5.9GHz$ |
| MAC protocol | *CSMA* |
| Transmission power $P$ | $1W$ |
| Noise floor $\kappa$ | $-100dB$ |
| Traffic intensity $\lambda_l$ | $0-30$ vehicles$/km$ |
| Decoding threshold $T$ | $0dB$ |
| Road Length $L$ | $10km$ |
| Inter-lane distance $d$ | $5m$ |
| Transmission range $R_t$ | $200m$ |
| Path loss exponent $\eta$ | 2 |

very close. In that case it is better to use the conservative approximation since it is computationally less intense. Moreover, it is evident that increasing the value of $\zeta$ improves the success probability which is according to expectations because a higher value of $\zeta$ provides more protection to the receiver from interference.

I now exploit the developed model to compare the normalized average forward progress made by the packets under the different transmission strategies described in Section 5.3. Note that in all the results, I use the aggressive approximation of the success probability since it is believed to be accurate under all values of $\zeta$. The result in Figure. 5.6 reveals several important characteristics. Firstly it is observed that for smaller sensing ranges, the *MFR* strategy suffers badly because of the smaller protection region from interference. It is also interesting to note that even for smaller sensing ranges, the *NFP* performs badly as compared to the *RFP*. However as the sensing range is increased to larger values, it is ultimately more beneficial to use the *MFR* forwarding strategy. Finally it can be seen that the relative advantage of selecting the best strategy increases with increasing traffic intensity.

Fig. 5.7 allows us to gain further insight into the system behaviour. The normalized average forward progress is plotted for the three transmission strategies against different values of $\lambda_l$ and also for different values of the sensing range to transmission

range ratio $\zeta$. It is clear that for smaller values of $\zeta$, the *RFP* strategy is the best for all traffic intensities. However increasing the value of $\zeta$ ultimately makes *MFR* the best performing strategy in terms of the normalized average progress. Exact critical values of $\zeta$ for the change of best strategy can be calculated from the intersecting points in Fig. 5.6. From Fig. 5.6 and Fig. 5.7, it is observed that the*NFP* performs poorly in terms of the normalized average forward progress for all traffic intensities and for larger values of $\zeta$.

### 5.7.2 Maximizing Transmission Capacity & Forward Progress

One of the key objectives in the design of IVC is to maximize the transmission capacity as well as maximizing the forward progress made by the packets. In other words I want to increase the number of successful parallel transmissions per unit length of road segment along with ensuring that I maximize the forward progress that is made under the transmissions. The result in Fig. 5.8 shows that there exists an optimal value of the design parameter $\rho_{th}$ that achieves the maximum transmission capacity and forward progress. It can be observed, in general, that the comparative advantage of the *MFR* strategy against the *NFP* increases as the traffic intensity increases. Secondly, it can be observed that the performance of the *NFP* strategy saturates as the intensity increases because of the small forward progress made despite the high success rate. Similarly, the performance of the *MFR* strategy also saturates with the increasing intensity because of the limit to the maximum progress that can be made despite the lower success rate. Moreover it can be observed that all the transmission strategies converge to the same performance as the transmission range increases (or equivalently, as the value of $\rho_{th}$ decreases).

## 5.8 Conclusion

The framework developed in this thesis is based on CSMA/CA protocol which allows a single transmitter inside a transmission range as opposed to ALOHA where there is no restriction on transmission. CSMA networks impose an inherent protection around a transmitter which prevents the receiver from interference whereas ALOHA networks suffer from massive interference. The protection in the CSMA protocol is controlled by the sensing threshold defined as $\rho_{th}$ in this thesis. The sensing threshold is a critical tuning parameter which can effect the probability of successful packet delivery and the number of simultaneously active transmitters in the network (which effects the spatial frequency reuse efficiency). For multi-hop communication, routing techniques also come into play to effectively disseminate packets across the network. A transmitter is required to select a transmission strategy for packet forwarding at every hop. For the overall system to be reliable and efficient (i.e. to meet particular QoS requirements), I need to maximize the progress made by packets at every step along with maximizing the success rate and the spatial frequency reuse efficiency. I develop a model based on stochastic geometry to accurately model the probability of success of the vehicle-to-vehicle communication system under different packet forwarding strategies and use that model to tune the sensing threshold of the CSMA MAC protocol.

# Chapter 6

# Conclusion

A novel analytical framework for modeling CSMA coordinated Inter-vehicle Communication in Multi-Lane Highways has been presented under both saturated and unsaturated transmission buffers. The developed model is based on stochastic geometry and point process theory. An approximate yet accurate expressions for the intensity of concurrent transmitters and packet success probability have been obtained. It has been shown that the single lane abstraction model is not always an accurate model and a comparison with other possible models is provided. The single lane abstraction model suffers mainly when the highway is very wide, i.e. more number of traffic lanes, or when the traffic intensity is high. Under these conditions, the proposed analysis is useful in evaluating the performance of IVC in a multi-lane highway. The The main conclusion is the fact that I show that the *MFR* transmission strategy is, overall better as compared to the other strategies in a multi-lane highway VANET. This is as opposed to the results given in [21] for general packet radio networks, where the authors show that the *NFP* strategy is better than the others. This difference is mainly due to the interference protection provided to the receiver by the CSMA protocol which allows for the improvement of the *MFR* performance. In the ALOHA setting used in [21], the receiver does not have any protection from the interferers and thus it is always better to transmit to the nearest available node to ultimately achieve higher progress.

# REFERENCES

[1] US Census Bureau. Available at: http://www.census.gov/compendia/statab/2012/tables/12s1104.pdf.

[2] National highway traffic safety administration. Available at: http://www-nrd.nhtsa.dot.gov/Pubs/812100.pdf.

[3] The cost of traffic jams. Available at: http://www.economist.com/blogs/economist-explains/2014/11/economist-explains-1.

[4] S. Yousefi, M. Mousavi, and M. Fathy, "Vehicular ad hoc networks (vanets): Challenges and perspectives," in *ITS Telecommunications Proceedings, 2006 6th International Conference on*, June 2006, pp. 761–766.

[5] C. Jiang, Y. Chen, and K. Liu, "Data-driven optimal throughput analysis for route selection in cognitive vehicular networks," *IEEE Journal on Selected Areas in Communications*, vol. 32, no. 11, pp. 2149–2162, November 2014.

[6] T. Willke, P. Tientrakool, and N. Maxemchuk, "A survey of inter-vehicle communication protocols and their applications," *IEEE Communications Surveys Tutorials*, vol. 11, no. 2, pp. 3–20, Second 2009.

[7] G. Karagiannis, O. Altintas, E. Ekici, G. Heijenk, B. Jarupan, K. Lin, and T. Weil, "Vehicular networking: a survey and tutorial on requirements, architectures, challenges, standards and solutions," *IEEE Communications Surveys Tutorials*, vol. 13, no. 4, pp. 584–616, Fourth 2011.

[8] F. F. Kuo, "The aloha system," *SIGCOMM Comput. Commun. Rev.*, vol. 25, no. 1, pp. 41–44, Jan. 1995. [Online]. Available: http://doi.acm.org/10.1145/205447.205451

[9] F. Tobagi, "Multiaccess protocols in packet communication systems," *Communications, IEEE Transactions on*, vol. 28, no. 4, pp. 468–488, Apr 1980.

[10] M. Haenggi, *Stochastic Geometry for Wireless Networks*. Cambridge University Press, 2012.

[11] H. Nguyen, F. Baccelli, and D. Kofman, "A stochastic geometry analysis of dense IEEE 802.11 networks," in *26th IEEE International Conference on Computer Communications.IEEE INFOCOM 2007.*, May 2007, pp. 1199–1207.

[12] M. Kaynia, N. Jindal, and G. Oien, "Improving the performance of wireless ad hoc networks through mac layer design," *IEEE Transactions on Wireless Communications*, vol. 10, no. 1, pp. 240–252, January 2011.

[13] H. ElSawy, E. Hossain, and S. Camorlinga, "Characterizing random csma wireless networks: A stochastic geometry approach," in *2012 IEEE International Conference on Communications (ICC)*, June 2012, pp. 5000–5004.

[14] M. Haenggi, *Stochastic geometry for wireless networks*. Cambridge University Press, 2012.

[15] M. Haenggi, J. Andrews, F. Baccelli, O. Dousse, and M. Franceschetti, "Stochastic geometry and random graphs for the analysis and design of wireless networks," *Selected Areas in Communications, IEEE Journal on*, vol. 27, no. 7, pp. 1029–1046, September 2009.

[16] P. Cardieri, "Modeling interference in wireless ad hoc networks," *Communications Surveys Tutorials, IEEE*, vol. 12, no. 4, pp. 551–572, Fourth 2010.

[17] M. Haenggi and R. K. Ganti, "Interference in large wireless networks," *Foundations and Trends in Networking*, vol. 3, no. 2, pp. 127–248, 2008. [Online]. Available: http://dx.doi.org/10.1561/1300000015

[18] F. Baccelli and B. Blaszczyszyn, *Stochastic Geometry and Wireless Networks, Volume I - Theory*, ser. Foundations and Trends in Networking Vol. 3: No 3-4, pp 249-449, F. Baccelli and B. Blaszczyszyn, Eds. NoW Publishers, 2009, vol. 1. [Online]. Available: https://hal.inria.fr/inria-00403039

[19] ——, *Stochastic Geometry and Wireless Networks, Volume II - Applications*, ser. Foundations and Trends in Networking Vol. 3: No 3-4, pp 249-449, F. Baccelli and B. Blaszczyszyn, Eds. NoW Publishers, 2009, vol. 1. [Online]. Available: https://hal.inria.fr/inria-00403039

[20] H. Takagi and L. Kleinrock, "Optimal transmission ranges for randomly distributed packet radio terminals," *Communications, IEEE Transactions on*, vol. 32, no. 3, pp. 246–257, Mar 1984.

[21] T.-C. Hou and V. Li, "Transmission range control in multihop packet radio networks," *IEEE Transactions on Communications*, vol. 34, no. 1, pp. 38–44, Jan 1986.

[22] C. Yin, L. Gao, T. Liu, and S. Cui, "Transmission capacities for overlaid wireless ad hoc networks with outage constraints," in *Communications, 2009. ICC '09. IEEE International Conference on*, June 2009, pp. 1–5.

[23] S. P. Weber, J. Andrews, X. Yang, and G. de Veciana, "Transmission capacity of wireless ad hoc networks with successive interference cancellation," *Information Theory, IEEE Transactions on*, vol. 53, no. 8, pp. 2799–2814, Aug 2007.

[24] J. Venkataraman, M. Haenggi, and O. Collins, "Shot noise models for outage and throughput analyses in wireless ad hoc networks," in *Military Communications Conference, 2006. MILCOM 2006. IEEE*, Oct 2006, pp. 1–7.

[25] H. ElSawy and E. Hossain, "A modified hard core point process for analysis of random csma wireless networks in general fading environments," *Communications, IEEE Transactions on*, vol. 61, no. 4, pp. 1520–1534, April 2013.

[26] M. Kaynia, N. Jindal, and G. Oien, "Improving the performance of wireless ad hoc networks through mac layer design," *Wireless Communications, IEEE Transactions on*, vol. 10, no. 1, pp. 240–252, January 2011.

[27] H. ElSawy, E. Hossain, and S. Camorlinga, "Multi-channel design for random csma wireless networks: A stochastic geometry approach," in *Communications (ICC), 2013 IEEE International Conference on*, June 2013, pp. 1656–1660.

[28] F. Baccelli, M. Klein, M. Lebourges, and S. Zuyev, "Stochastic geometry and architecture of communication networks," *Telecommunication Systems*, vol. 7, no. 1-3, pp. 209–227, 1997. [Online]. Available: http://dx.doi.org/10.1023/A%3A1019172312328

[29] T. Brown, "Cellular performance bounds via shotgun cellular systems," *Selected Areas in Communications, IEEE Journal on*, vol. 18, no. 11, pp. 2443–2455, Nov 2000.

[30] H. Dhillon, R. Ganti, F. Baccelli, and J. Andrews, "Modeling and analysis of k-tier downlink heterogeneous cellular networks," *Selected Areas in Communications, IEEE Journal on*, vol. 30, no. 3, pp. 550–560, April 2012.

[31] H. Dhillon, T. Novlan, and J. Andrews, "Coverage probability of uplink cellular networks," in *Global Communications Conference (GLOBECOM), 2012 IEEE*, Dec 2012, pp. 2179–2184.

[32] D. Jiang and L. Delgrossi, "Ieee 802.11p: Towards an international standard for wireless access in vehicular environments," in *Vehicular Technology Conference, 2008. VTC Spring 2008. IEEE*, May 2008, pp. 2036–2040.

[33] L. Stibor, Y. Zang, and H.-J. Reumerman, "Evaluation of communication distance of broadcast messages in a vehicular ad-hoc network using ieee 802.11p," in *Wireless Communications and Networking Conference, 2007.WCNC 2007. IEEE*, March 2007, pp. 254–257.

[34] B. Gukhool and S. Cherkaoui, "Ieee 802.11p modeling in ns-2," in *Local Computer Networks, 2008. LCN 2008. 33rd IEEE Conference on*, Oct 2008, pp. 622–626.

[35] T. Murray, T. Murray, M. Cojocari, and H. Fu, "Measuring the performance of ieee 802.11p using ns-2 simulator for vehicular networks," in *Electro/Information Technology, 2008. EIT 2008. IEEE International Conference on*, May 2008, pp. 498–503.

[36] B. Blaszczyszyn, P. Muhlethaler, and Y. Toor, "Maximizing throughput of linear vehicular ad-hoc neworks (vanets) ; a stochastic approach," in *European Wireless Conference, 2009*, May 2009, pp. 32–36.

[37] B. Baszczyszyn, P. Mhlethaler, and Y. Toor, "Stochastic analysis of aloha in vehicular ad hoc networks," *Annals of Telecommunications*, vol. 68, no. 1-2, pp. 95–106, 2013. [Online]. Available: http://dx.doi.org/10.1007/s12243-012-0302-2

[38] J. Harri, F. Filali, and C. Bonnet, "Mobility models for vehicular ad hoc networks: a survey and taxonomy," *Communications Surveys Tutorials, IEEE*, vol. 11, no. 4, pp. 19–41, Fourth 2009.

[39] C. Sommer, Z. Yao, R. German, and F. Dressler, "On the need for bidirectional coupling of road traffic microsimulation and network simulation," in *Proceedings of the 1st ACM SIGMOBILE Workshop on Mobility Models*, ser. MobilityModels '08. New York, NY, USA: ACM, 2008, pp. 41–48. [Online]. Available: http://doi.acm.org/10.1145/1374688.1374697

[40] A. Giang and A. Busson, "Modeling csma/ca in vanet," in *Analytical and stochastic modeling techniques and applications*, ser. Lecture Notes in Computer Science, K. Al-Begain, D. Fiems, and J.-M. Vincent, Eds. Springer Berlin Heidelberg, 2012, vol. 7314, pp. 91–105. [Online]. Available: http://dx.doi.org/10.1007/978-3-642-30782-9_7

[41] T. Nguyen, F. Baccelli, K. Zhu, S. Subramanian, and X. Wu, "A performance analysis of csma based broadcast protocol in vanets," in *IEEE INFOCOM 2013*, April 2013, pp. 2805–2813.

[42] M. Kaynia, N. Jindal, and G. Oien, "Performance of vehicle-to-vehicle communication using ieee 802.11p in vehicular ad-hoc network environment," *International Journal of Network Security and Its Applications (IJNSA)*, vol. 5, no. 2, 2013.

[43] Y. Yao, L. Rao, and X. Liu, "Performance and reliability analysis of ieee 802.11p safety communication in a highway environment," *IEEE Transactions on Vehicular Technology*, vol. 62, no. 9, pp. 4198–4212, Nov 2013.

[44] A. Souza, A. L. Barros, A. S. Vieira, F. Roberto, and J. C. Júnior, "An adaptive mechanism for access control in vanets," in *The Tenth International Conference on Networks (ICN) 2011*, 2011, pp. 183–188.

[45] R. Stanica, E. Chaput, and A.-L. Beylot, "Enhancements of ieee 802.11 p protocol for access control on a vanet control channel," in *2011 IEEE International Conference on Communications (ICC)*, 2011, pp. 1–5.

[46] S. Eichler, "Performance evaluation of the IEEE 802.11p wave communication standard," in *IEEE 66th Vehicular Technology Conference (VTC-Fall 2007)*, September 2007, pp. 2199–2203.

[47] S. P. Weber, X. Yang, J. Andrews, and G. de Veciana, "Transmission capacity of wireless ad hoc networks with outage constraints," *IEEE Transactions on Information Theory*, vol. 51, no. 12, pp. 4091–4102, Dec 2005.

[48] R. P. Roess, E. S. Prassas, and W. R. McShane, "Traffic engineering," *NJ: Prentice-Hall*, 2004.

[49] A. Alfa, *Queueing theory for telecommunications: discrete time modelling of a single node system.* Springer, 2010.

[50] L. Sartori, S.-E. Elayoubi, B. Fourestie, and Z. Nouir, "On the WiMAX and HSDPA coexistence," in *IEEE International Conference on Communications, 2007. ICC '07.*, June 2007, pp. 5636–5641.

[51] H. Takagi and L. Kleinrock, "Optimal transmission ranges for randomly distributed packet radio terminals," *IEEE Transactions on Communications*, vol. 32, no. 3, pp. 246–257, 1984.

# APPENDICES

# A Proof of Lemma 1

Following the PPP definitions, the vehicles are uniformly distributed over the traffic lanes. Hence, from the length of the traffic chord, the *pdf* of the horizontal distance between the origin and the selected transmitter (c.f. Fig. 3.4) is given by

$$f_X(x) = \frac{1}{\sqrt{r^2 - (md)^2}}, \qquad 0 \leq x \leq \sqrt{r^2 - (md)^2}. \tag{A.1}$$

Since the distance $r_o$ is related to $X$ via Pythagoras theorem, **Lemma 1** can be directly obtained.

# B Proof of Lemma 2

The same-lane neighborhood set for a generic vehicle can be described as: $|\mathcal{N}_{v_{ij}}| = \sum_{v_{ij}\in\mathbf{\Phi}_i\setminus v_o} \mathbb{1}_{\{Ph_{ij}\|v_{ij}\|^{-\eta}>\rho_{th}\}}$, where $\mathbb{1}_{\{.\}}$ is the indicator function. The moment generating function of $|\mathcal{N}_{v_{ij}}|$ can be expressed as:

$$\begin{aligned}
\mathbb{E}\left[\exp\left\{t|\mathcal{N}|\right\}\right] &= \mathbb{E}\left[\exp\left(t\sum_{v_{ij}\in\Phi_i}\mathbb{1}_{\{Ph_{ij}\|v_{ij}\|^{-\eta}>\rho_{th}\}}\right)\right] \\
&= \mathbb{E}_{\Phi}\left[\prod_{v_{ij}\in\Phi_i}\mathbb{E}_{h_{ij}}\left[e^{t\mathbb{1}_{\{Ph_{ij}\left\|v_{ij}\right\|^{-\eta}>\rho_{th}\}}}\right]\right] \\
&\overset{(i)}{=} \exp\left\{-\mathbb{E}_h\left[\int_0^{\left(\frac{Ph}{\rho_{th}}\right)^{\frac{1}{\eta}}}(1-e^t)\lambda_l dr\right]\right\} \\
&= \exp\left\{(e^t-1)\lambda_l\left(\frac{P}{\mu\rho_{th}}\right)^{\frac{1}{\eta}}\Gamma(\frac{1}{\eta}+1)\right\} \qquad \text{(B.1)}
\end{aligned}$$

where $(i)$ follows from the probability generation functional (PGFL) of the PPP. Note that the integration boundaries in $(i)$ implies that we consider only one side of the contention domain. Equation (B.1) is the moment generating function of a poisson process with mean, $\mathbb{E}\left[|\mathcal{N}|\right] = \lambda_l\left(\frac{P}{\mu\rho_{th}}\right)^{\frac{1}{\eta}}\Gamma(\frac{1}{\eta}+1)$.

# C Proof of Theorem 1

For the case of a single lane highway, the LT of the aggregate interference can be expressed as:

$$\begin{aligned}\mathcal{L}_I(s) &= \mathbb{E}_{\tilde{\Phi}}\{e^{-sI}\} = \mathbb{E}_{\tilde{\Phi}}\left[\exp\left(-s\sum_{v_{1j}\in\tilde{\Phi}\setminus v_0} Ph_{1j}\|v_{1j}\|^{-\eta}\right)\right] \\ &= \mathbb{E}_{\tilde{\Phi}}\left[\prod_{j\in\tilde{\Phi}}\mathcal{L}_h(sP\|v_{1j}\|^{-\eta})\right] \overset{(i)}{=} \mathbb{E}_{\tilde{\Phi}}\left[\prod_{j\in\tilde{\Phi}}\frac{\mu}{\mu+sP\|v_{1j}\|^{-\eta}}\right] \\ &\overset{(ii)}{=} \exp\left(-\Lambda\int_{\mathbb{R}^1}\left(1-\frac{\mu}{\mu+Ps\gamma^{-\eta}}\right)d\gamma\right) \\ &= \exp\left(-\Lambda\left(\frac{Ps}{\mu}\right)^{\frac{1}{\eta}}\int_{\mathbb{R}^1}\frac{1}{1+t^{\eta}}dt\right) \end{aligned} \tag{C.1}$$

where $(i)$ follows from the LT of the exponential distribution and $(ii)$ follows from the PGFL of a PPP. Substituting (C.1) in (3.2) and putting appropriate limits of integration for the interference region proves the theorem.

# D Proof of Theorem 2

For a multi-lane highway, the LT of the aggregate interference can be expressed as:

$$\begin{aligned}
\mathcal{L}_I(s) &= \mathbb{E}_{\tilde{\Phi}_i}\{e^{-sI}\} = \mathbb{E}_{\tilde{\Phi}_i}\left[\exp\left(-s\sum_{i=1}^{N}\sum_{v_{ij}\in\tilde{\Phi}_i\setminus v_0} Ph_{ij}\|v_{ij}\|^{-\eta}\right)\right] \\
&= \prod_{i=1}^{N}\mathbb{E}_{\tilde{\Phi}_i}\left[\prod_{j\in\tilde{\Phi}_i}\mathcal{L}_h(sP\|v_{ij}\|^{-\eta})\right] \\
&\overset{(a)}{=} \prod_{i=1}^{N}\mathbb{E}_{\tilde{\Phi}_i}\left[\prod_{j\in\tilde{\Phi}_i}\frac{\mu}{\mu+sP\|v_{ij}\|^{-\eta}}\right] \\
&\overset{(b)}{=} \prod_{i=-(N-1)/2}^{(N-1)/2}\exp\left(-\int_{\psi_i\in R^1}\tilde{\Lambda}(\gamma_i,i)\left(1-\frac{\mu}{\mu+Ps\gamma_i^{-\eta}}\right)d\gamma_i\right) \\
&= \prod_{i=-(N-1)/2}^{(N-1)/2}\exp\left(-\int_{\psi_i\in R^1}\left(\frac{\tilde{\Lambda}(\gamma_i,i)Ps\gamma_i^{-\eta}}{\mu+Ps\gamma_i^{-\eta}}\right)d\gamma_i\right) \qquad \text{(D.1)}
\end{aligned}$$

where $(a)$ follows from the LT of the exponential distribution and $(b)$ follows from the PGFL of a PPP. $\psi_i$ represents the interference region on the $i^{th}$ traffic lane. Thus the limits of integration are from $\hat{\gamma}_i$ to $\infty$ and $-\infty$ to $\tilde{\gamma}_i$ as shown in Fig. 3.8. Substituting (D.1) in (3.2) proves the theorem.

# E Proof of Lemma 7

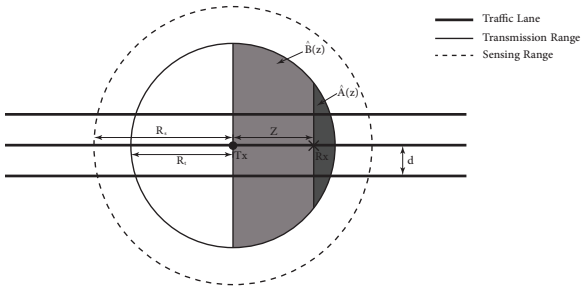


Figure E.1: Transmitter-Receiver distance for MFR strategy

Let $X+$ be the event that there exists a receiver inside the forward transmission range, illustrated by the shaded half circle in Fig.E.1, of the test transmitter. The probability of the event can be calculated as follows:

$$\begin{aligned}\mathbb{P}\left[X+\right] &= \mathbb{P}\left[\text{At least one vehicle in } \{\hat{\mathbf{A}}(\mathrm{z}) + \hat{\mathbf{B}}(\mathrm{z})\}\right] \\ &= 1 - \mathbb{P}\left[\text{No vehicle in } \{\hat{\mathbf{A}}(\mathrm{z}) + \hat{\mathbf{B}}(\mathrm{z})\}\right] \\ &= 1 - e^{-\mathbb{E}[|\mathbf{N}|]/2}, \end{aligned} \tag{E.1}$$

where $\mathbb{E}\left[|\mathbf{N}|\right]/2$ is the average number of forward neighbours of the transmitter. Now let $\mathrm{Z}_\chi$ be a random variable denoting the forward progress made by the packet in one transmission. The subscript $\chi \in \{\mathrm{M,N,R}\}$ referring to the *MFR,NFP* and *RFP* strategy respectively. Using the methodology in [21], the conditional CDF of Z

can be expressed as follows:

$$\begin{aligned} F_{\mathrm{Z_M}}(\mathrm{z}|\mathrm{X}+) &= \mathbb{P}\{\mathrm{Z_M} \le \mathrm{z}|\mathrm{X}+\} = \frac{\mathbb{P}\{\text{No vehicle in } \hat{\mathbf{A}}(\mathrm{z}) \text{ and X}+\}}{\mathbb{P}\{\mathrm{X}+\}} \\ &= \frac{\mathbb{P}\{\text{No vehicle in } \hat{\mathbf{A}}(\mathrm{z}) \text{ and at least one vehicle in } \hat{\mathbf{B}}(\mathrm{z})}{\mathbb{P}\{X+\}} \\ &= \frac{\mathbb{P}\{\text{No vehicle in } \hat{\mathbf{A}}(\mathrm{z})\}\mathbb{P}\{\text{At least one vehicle in } \hat{\mathbf{B}}(\mathrm{z})}{\mathbb{P}\{X+\}} \\ &= \frac{e^{-\lambda_l \mathbf{A}(\mathrm{z})}(1-e^{-\lambda_l \mathbf{B}(\mathrm{z})})}{1-e^{-\mathbb{E}[|\mathbf{N}|]/2}} \\ &= \frac{e^{-\lambda_l \mathbf{A}(\mathrm{z})} - e^{-\mathbb{E}[|\mathbf{N}|]/2}}{1-e^{-\mathbb{E}[|\mathbf{N}|]/2}} \qquad 0 \le z \le R_t \end{aligned} \tag{E.2}$$

where $\hat{\mathbf{A}}(\mathrm{z})$ is the shaded region illustrated in Fig.E.1 and the length of road segment inside the shaded region, denoted by $\mathbf{A}(\mathrm{z})$, is given by:

$$\mathbf{A}(\mathrm{z}) = \begin{cases} \frac{\mathbb{E}[|\mathbf{N}|]}{2\lambda_l} - N\mathrm{z}, & 0 < \mathrm{z} \le \sqrt{R_t^2 - (\frac{N-1}{2}d)^2} \\ \frac{\mathbb{E}[|\mathbf{N}|]}{2\lambda_l} - 2\sqrt{R_t^2 - (\frac{N-1}{2}d)^2} - (N-2)\mathrm{z}, & \\ \qquad \sqrt{R_t^2 - (\frac{N-1}{2}d)^2} < \mathrm{z} \le \sqrt{R_t^2 - (\frac{N-3}{2}d)^2} & \\ \qquad\qquad \vdots & \\ \frac{\mathbb{E}[|\mathbf{N}|]}{2\lambda_l} - 2\sum\limits_{i=1}^{\frac{N-1}{2}} \sqrt{R_t^2 - (\frac{N-(2i-1)}{2}d)^2} - \mathrm{z}. & \\ \qquad\qquad \sqrt{R_t^2 - d^2} < \mathrm{z} \le R_t & \end{cases} \tag{E.3}$$

For the case when $R_t >> \frac{(N-1)d}{2}$, $\mathbf{A}(\mathrm{z})$ can be approximately expressed as:

$$\mathbf{A}(\mathrm{z}) \approx \frac{\mathbb{E}[|\mathbf{N}|]}{2\lambda_l} - N\mathrm{z}, \quad 0 \le \mathrm{z} \le \mathrm{R_t} \tag{E.4}$$

The conditional probability distribution of forward progress Z can then be evaluated by taking the derivative of (E.2):

$$\begin{aligned} f_{\mathrm{Z_M}}(\mathrm{z}|\mathrm{X}+) &= \frac{-\lambda_l e^{-\lambda_l \mathbf{A}(\mathrm{z})}}{1-e^{-\mathbb{E}[|\mathbf{N}|]/2}} \times \frac{d\mathbf{A}(\mathrm{z})}{dz} \\ &= \frac{N\lambda_l e^{-\lambda_l(\mathbb{E}[|\mathbf{N}|]/2 - Nz)}}{1-e^{-\mathbb{E}[|\mathbf{N}|]/2}} \qquad 0 \le z \le R_t \end{aligned} \tag{E.5}$$

For a test transmitter at the origin, a potential receiver can be located either on the same traffic lane or on an adjacent lane. If the receiver is on the same lane, the

conditional pdf can be written as:

$$f_{r_M}(r|l_0) = f_{\mathrm{Z}_M}(r) = \frac{N\lambda_l e^{-\lambda_l \mathbf{A}(r)}}{1 - e^{\mathbb{E}[|\mathbf{N}|/2]}} \qquad 0 \le r \le R_t \tag{E.6}$$

If the receiver is located on the $i^{th}$ adjacent traffic lane, the conditional pdf $f_{r_M}(z|l_i)$ for $i = 1 \ldots (N-1)/2$, can be obtained using the following procedure:

$$\begin{aligned} r_M &= z^2 + (id)^2 \\ F_{r_M}(r|l_i) &= \mathbb{P}(r_M \le r) = \mathbb{P}(\sqrt{z^2 + (id)^2} \le r) \\ &= \mathbb{P}(z \le \sqrt{r^2 - (id)^2}) = F_z(\sqrt{r^2 - (id)^2}) \\ &= \frac{\exp\left(-\lambda_l \mathbf{A}(\sqrt{r^2 - (id)^2})\right) - \exp\left(-\mathbb{E}\left[|\mathbf{N}|\right]/2\right)}{1 - e^{-\mathbb{E}[|\mathbf{N}|]/2}} \end{aligned} \tag{E.7}$$

From (E.7), we can obtain the conditional pdf as:

$$f_{r_M}(r|l_i) = \frac{N\lambda_l r \exp\left(-\lambda_l \mathbf{A}(\sqrt{r^2 - (id)^2})\right)}{(1 - e^{-\mathbb{E}[|\mathbf{N}|]/2})\sqrt{r^2 - (id)^2}} \qquad d \le r \le R_t \tag{E.8}$$

Finally the complete pdf of the transmitter-receiver distance $r_M$ can be obtained as follows:

$$f_{r_M}(r) = \begin{cases} \frac{\lambda_l e^{-\lambda_l \mathbf{A}(r)}}{1 - e^{\mathbb{E}[|\mathbf{N}|/2]}} & 0 < r \le d \\ \frac{\lambda_l e^{-\lambda_l \mathbf{A}(r)}}{1 - e^{\mathbb{E}[|\mathbf{N}|/2]}} + \frac{2\lambda_l r \exp\left(-\lambda_l \mathbf{A}\left(\sqrt{r^2 - d^2}\right)\right)}{(1 - e^{\mathbb{E}[|\mathbf{N}|/2]})\sqrt{r^2 - d^2}} & d < r \le 2d \\ \quad \vdots & \\ \frac{\lambda_l e^{-\lambda_l \mathbf{A}(r)}}{1 - e^{\mathbb{E}[|\mathbf{N}|/2]}} + & \\ \quad \sum_{i=1}^{(N-1)/2} \frac{2\lambda_l r \exp\left(-\lambda_l \mathbf{A}\left(\sqrt{r^2 - (id)^2}\right)\right)}{(1 - e^{\mathbb{E}[|\mathbf{N}|/2]})\sqrt{r^2 - (id)^2}} \cdot & \frac{(N-1)d}{2} < r \le R_t \end{cases} \tag{E.9}$$

For the MFR strategy, the value of $r_M$ is close to $R_t$ with high probability. Hence

the pdf can be reasonably approximated (for high traffic intensities) as:

$$f_{r_M}(r) \approx \begin{cases} 0 & 0 < r \leq \frac{(N-1)d}{2} \\ \frac{\lambda_l e^{-\lambda_l \mathbf{A}(r)}}{1-e^{\mathbb{E}[|\mathbf{N}|/2]}} + & \\ \sum_{i=1}^{(N-1)/2} \frac{2\lambda_l r e^{-\lambda_l \mathbf{A}\left(\sqrt{r^2-(id)^2}\right)}}{(1-e^{\mathbb{E}[|\mathbf{N}|/2]})\sqrt{r^2-(id)^2}}. & \frac{(N-1)d}{2} < r \leq R_t \end{cases}$$

# F Proof of Lemma 8

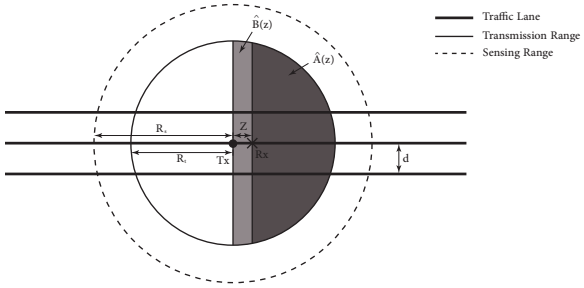


Figure F.1: Transmitter-Receiver distance for NFP strategy

Similar to the proof in Appendix E, we can derive the pdf for the *NFP* case as follows:

$$\begin{aligned} F_{\mathrm{Z_N}}(\mathrm{z}|\mathrm{X}+) &= \frac{\mathbb{P}\{\text{No vehicle in } \hat{\mathbf{B}}(\mathrm{z})\}\mathbb{P}\{\text{At least one vehicle in } \hat{\mathbf{A}}(\mathrm{z})}{\mathbb{P}\{X+\}} \\ &= \frac{e^{-\lambda_l \mathbf{B}(\mathrm{z})} - e^{-\mathbb{E}[|\mathbf{N}|]/2}}{1 - e^{-\mathbb{E}[|\mathbf{N}|]/2}} \qquad 0 \le z \le R_t \end{aligned} \tag{F.1}$$

where $\mathbf{B}(\mathrm{z})$ is the length of road segment inside the shaded region $\hat{\mathbf{B}}(\mathrm{z})$ illustrated in Fig. F.1, and is expressed as:

$$\mathbf{B}(\mathrm{z}) = \begin{cases} N\mathrm{z}, & 0 < \mathrm{z} \le \sqrt{R_t^2 - (\frac{N-1}{2}d)^2} \\ 2\sqrt{R_t^2 - (\frac{N-1}{2}d)^2} + (N-2)\mathrm{z}, & \\ \qquad \sqrt{R_t^2 - (\frac{N-1}{2}d)^2} < \mathrm{z} \le \sqrt{R_t^2 - (\frac{N-3}{2}d)^2} & \\ \qquad \vdots & \\ 2\sum_{i=1}^{\frac{N-1}{2}} \sqrt{R_t^2 - (\frac{N-(2i-1)}{2}d)^2} + \mathrm{z}. & \\ \qquad \sqrt{R_t^2 - d^2} < \mathrm{z} \le R_t \end{cases} \tag{F.2}$$

For the case when $R_t >> \frac{(N-1)d}{2}$, B(z) can be approximately expressed as:

$$\mathbf{B}(\mathrm{z}) \approx N\mathrm{z} \tag{F.3}$$

The approximate *pdf* of the forward progress in the *NFP* case is therefore given as:

$$f_{\mathrm{Z}_N}(\mathrm{z}) = \frac{N\lambda_l e^{-\lambda_l N\mathrm{z}}}{1 - e^{\mathbb{E}[|\mathbf{N}|/2]}} \qquad 0 \leq r \leq R_t \tag{F.4}$$

Using the same procedure as before, the probability distribution for the transmitter-receiver distance $r_N$ can be obtained as follows:

$$f_{r_N}(r) = \begin{cases} \frac{\lambda_l e^{-\lambda_l \mathbf{B}(r)}}{1-e^{\mathbb{E}[|\mathbf{N}|/2]}} & 0 \leq r \leq d \\ \frac{\lambda_l e^{-\lambda_l \mathbf{B}(r)}}{1-e^{\mathbb{E}[|\mathbf{N}|/2]}} + \frac{2\lambda_l r \exp\left(-\lambda_l \mathbf{B}\left(\sqrt{r^2-d^2}\right)\right)}{(1-e^{\mathbb{E}[|\mathbf{N}|/2]})\sqrt{r^2-d^2}} & d < r \leq 2d \\ \vdots & \\ \frac{\lambda_l e^{-\lambda_l \mathbf{B}(r)}}{1-e^{\mathbb{E}[|\mathbf{N}|/2]}} + \sum_{i=1}^{(N-1)/2} \frac{2\lambda_l r \exp\left(-\lambda_l \mathbf{B}\left(\sqrt{r^2-(id)^2}\right)\right)}{(1-e^{\mathbb{E}[|\mathbf{N}|/2]})\sqrt{r^2-(id)^2}}, & \frac{(N-1)d}{2} < r \leq R_t \end{cases} \tag{F.5}$$

Fortunately, for the NFP case, there is a high probability of the receiver being located very close to the transmitter and on the same lane as the transmitter. Hence we can reasonably approximate the pdf of $r_N$ as follows:

$$f_{r_N}(r) \approx \frac{N\lambda_l e^{-\lambda_l Nr}}{1 - e^{\mathbb{E}[|\mathbf{N}|/2]}} \qquad 0 < r \leq R_t \tag{F.6}$$

The average distance between any two closest nodes, using the approximation in (F) is given as:

$$\mathbb{E}[r_N] = \int_0^\infty r f_{r_N} dr = \frac{1}{N\lambda_l} \tag{F.7}$$

# G Proof of Lemma 9

For the RFP strategy, the relay node can be any of the vehicles in the forward neighbourhood of the transmitter. The transmitter-receiver distance is distributed as follows:

$$f_{r_R}(r) = \begin{cases} \frac{1}{NR_t}, & 0 \le r \le d \\ \frac{1}{NR_t} + \frac{2r}{NR_t\sqrt{r^2-d^2}}, & d < r \le 2d \\ \quad\vdots & \\ \frac{1}{NR_t} + \sum_{i=1}^{(N-1)/2} \frac{2r}{NR_t\sqrt{r^2-(id)^2}}, & \frac{(N-1)d}{2} < r \le R_t. \end{cases} \tag{G.1}$$

The probability distribution of the forward progress in the case of the *RFP* strategy, denoted by $\mathrm{Z}_R$, is given as:

$$f_{\mathrm{Z}_R}(z) = \begin{cases} \frac{1}{NR_t} + \sum_{i=1}^{(N-1)/2} \frac{2}{N\sqrt{R_t^2-(id)^2}}, & \\ \qquad\qquad 0 \le z \le \sqrt{R_t^2 - \left(\frac{(N-1)d}{2}\right)^2} & \\ \frac{1}{NR_t} + \sum_{i=1}^{(N-3)/2} \frac{2}{N\sqrt{R_t^2-(id)^2}}, & \\ \sqrt{R_t^2 - \left(\frac{(N-1)d}{2}\right)^2} < z \le \sqrt{R_t^2 - \left(\frac{(N-3)d}{2}\right)^2} & \\ \quad\vdots & \\ \frac{1}{NR_t}, \qquad\qquad \sqrt{R_t^2 - d^2} < z \le R_t. \end{cases} \tag{G.2}$$

If $R_t >> \frac{(N-1)d}{2}$, $f_{\mathrm{Z}_R}(z)$ can be approximated as:

$$f_{\mathrm{Z}_R}(z) \approx \frac{1}{R_t}, \quad 0 \le z \le R_t \tag{G.3}$$

# H Proof of Average Forward Progress

The proof of the average forward progress $\mathrm{Z}_\chi$ is done by simply taking the expectation of the forward progress for each transmission strategy. The distribution of the forward progress is given in (E.6), (F.4) and (G.2) respectively. For notational convenience, we define the function $\omega$ which is defined as:

$$\omega(i) = \sqrt{R_t^2 - \left(\frac{N-(2i-1)}{2}d\right)^2} \tag{H.1}$$

The average forward progress for the *MFR* strategy is evaluated as follows:

$$\begin{aligned}\mathbb{E}[\mathrm{Z}_M] = \int_0^{R_t} z f_{Z_M}(z)dz = \int_0^{\omega(1)} zN\lambda_l e^{-\lambda_l(\frac{\mathbb{E}[|\mathbf{N}|]}{2\lambda_l}-Nz)}dz + \int_{\omega(1)}^{\omega(2)} zN\lambda_l e^{-\lambda_l\left(\frac{\mathbb{E}[|\mathbf{N}|]}{2\lambda_l}-2\omega(1)-(N-2)z\right)}dz \\ + \quad \ldots \quad + \int_{\omega(\frac{N-1}{2})}^{R_t} zN\lambda_l e^{-\lambda_l\left(\frac{\mathbb{E}[|\mathbf{N}|]}{2\lambda_l}-2\sum_{i=1}^{\frac{N-1}{2}}\omega(i)\ -\ z\right)}dz\end{aligned} \tag{H.2}$$

Similarly, the average forward progress for the *NFP* and *RFP* strategies is evaluated as follows:

$$\mathbb{E}[\mathrm{Z}_N] = \int_0^{R_t} z f_{Z_N}(z)dz = \int_0^{\omega(1)} zN\lambda_l e^{-\lambda_l N z}dz \; + \int_{\omega(1)}^{\omega(2)} zN\lambda_l e^{-\lambda_l(2\omega(1)+(N-2)z)}dz \quad + \quad \ldots \quad +$$
$$\int_{\omega(\frac{N-1}{2})}^{R_t} zN\lambda_l e^{-\lambda_l\left(2\sum_{i=1}^{\frac{N-1}{2}}\omega(i)\,+\,z\right)}dz. \tag{H.3}$$

$$\mathbb{E}[\mathrm{Z}_R] = \int_0^{\omega(1)} z\left(\frac{1}{NR_t} + \frac{2}{N}\sum_{i=1}^{(N-1)/2}\frac{1}{\sqrt{R_t^2-(id)^2}}\right)dz +$$
$$\int_{\omega(1)}^{\omega(2)} z\left(\frac{1}{NR_t} + \frac{2}{N}\sum_{i=1}^{(N-3)/2}\frac{1}{\sqrt{R_t^2-(id)^2}}\right)dz$$
$$+ \quad \ldots \quad + \int_{\omega(\frac{N-1}{2})}^{R_t} \frac{z}{NR_t}dz \tag{H.4}$$

These integrals are easy to evaluate and it is straightforward to show that they can be simplified to obtain the expressions in (5.13), (5.14) and (5.15).

# I Papers Submitted

• Muhammad Junaid Farooq, Hesham ElSawy, and Mohamed-Slim Alouini, "Modeling Inter-vehicle Communication in Multi-lane Highways: A Stochastic Geometry Approach", *Submitted to IEEE VTC Fall 2015*, Boston.

• Muhammad Junaid Farooq, Hesham ElSawy, and Mohamed-Slim Alouini, "A Stochastic Geometry Model for Multi-hop Highway Vehicular Communication", *Submitted to IEEE Transactions on Wireless Communication (TWC)*, Feb. 2015.